J|A|C|S ARTICLES

Published on Web 07/06/2009

Length-Dependent Convergence and Saturation Behavior of Electrochemical, Linear Optical, Quadratic Nonlinear Optical, and Cubic Nonlinear Optical Properties of Dipolar Alkynylruthenium Complexes with Oligo(phenyleneethynylene) Bridges

Bandar Babgi,[†] Luca Rigamonti,[†,‡] Marie P. Cifuentes,[†] T. Christopher Corkery,[†] Michael D. Randles,[†] Torsten Schwich,[†] Simon Petrie,[†] Robert Stranger,[†] Ayele Teshome,[§] Inge Asselberghs,[§] Koen Clays,[§] Marek Samoc,[⊥,△] and Mark G. Humphrey*[,†]

Research School of Chemistry, Australian National University, Canberra, ACT 0200, Australia, Dipartimento di Chimica Inorganica, Metallorganica e Analitica 'Lamberto Malatesta', Università degli Studi di Milano, Via Venezian 21, 20133 Milano, Italy, Department of Chemistry, University of Leuven, Celestijnenlaan 200D, B-3001 Leuven, Belgium, Laser Physics Centre, Research School of Physics and Engineering, Australian National University, Canberra, ACT 0200, Australia, and Institute of Physical and Theoretical Chemistry, Wroclaw University of Technology, 50-370 Wroclaw, Poland

Received April 7, 2009; E-mail: Mark.Humphrey@anu.edu.au

Abstract: The syntheses of *trans*-[Ru{4,4′-C≡CC_6H_2[2,5-$(OEt)_2$]C≡$CC_6H_4NO_2$}Cl$(dppm)_2$] (**19**), *trans*-[Ru{4,4′,4″-C≡CC_6H_4C≡CC_6H_2[2,5-$(OEt)_2$]C≡$CC_6H_4NO_2$}Cl$(dppm)_2$] (**20**), *trans*-[Ru{4,4′,4″,4‴-C≡CC_6H_4-C≡CC_6H_2[2,5-$(OEt)_2$]C≡CC_6H_2[2,5-$(OEt)_2$]C≡$CC_6H_4NO_2$}Cl$(dppe)_2$] (**21**), *trans*-[Ru{4,4′,4″,4‴-C≡CC_6H_4-C≡CC_6H_2[2,5-$(OEt)_2$]C≡CC_6H_2[2,5-$(OEt)_2$]C≡$CC_6H_4NO_2$}Cl$(dppm)_2$] (**22**), *trans*-[Ru{4,4′,4″,4‴-C≡CC_6H_4C≡CC_6H_4C≡CC_6H_2[2,5-$(OEt)_2$]C≡$CC_6H_4NO_2$}Cl$(dppm)_2$] (**23**), and *trans*-[Ru{4,4′,4″,4‴,4⁗-C≡CC_6H_4-C≡CC_6H_4C≡CC_6H_2[2,5-$(OEt)_2$]C≡CC_6H_2[2,5-$(OEt)_2$]C≡$CC_6H_4NO_2$}Cl$(dppm)_2$] (**24**) are reported, together with those of precursor alkynes, complexes with the donor−π-bridge−acceptor formulation that affords efficient quadratic and cubic NLO compounds; the identity of **19** was confirmed by a structural study. The electrochemical properties of **19**−**24** and related complexes with shorter π-bridge ligands were assessed by cyclic voltammetry, and the linear optical, quadratic nonlinear optical, and cubic nonlinear optical properties were assayed by UV−vis−NIR spectroscopy, hyper-Rayleigh scattering studies at 1064 and 1300 nm, and broad spectral range femtosecond Z-scan studies, respectively. The $Ru^{II/III}$ oxidation potentials and wavelengths of the optical absorption maxima decrease on π-bridge lengthening, until the tri(phenyleneethynylene) complex is reached, further chain lengthening leaving these parameters invariant; theoretical studies employing time-dependent density functional theory have shed light on this behavior. The quadratic nonlinearity β_{1064} and two-photon absorption cross-section reach maximal values at this same π-bridge length, a similar saturation behavior that may reflect a common importance of ruthenium-to-alkynyl ligand charge transfer in electronic and optical behavior in these molecules.

Introduction

Considerable interest has been shown in the nonlinear optical (NLO) properties of organometallic complexes,[1−6] with the majority of studies involving propagation of structure−property relationships developed in organic systems into the organometallic domain. Organic compounds with a donor−π-bridge−acceptor composition were shown to possess large quadratic NLO properties that could be enhanced by increasing donor or acceptor strength or by bridge modification,[7] while compounds with extended π-systems were shown to possess

[†] RSC, Australian National University.
[‡] Università degli Studi di Milano.
[§] University of Leuven.
[⊥] RSPE, Australian National University.
[△] Wroclaw University of Technology.

(1) Organometallic Complexes for Nonlinear Optics. Part 44. Part 43: Rigamonti, L.; Babgi, B.; Cifuentes, M. P.; Roberts, R. L.; Petrie, S.; Stranger, R.; Righetto, S.; Teshome, A.; Asselberghs, I.; Clays, K.; Humphrey, M. G. *Inorg. Chem.* **2009**, *48*, 3562.
(2) Long, N. J. *Angew. Chem., Int. Ed. Engl.* **1995**, *34*, 21.
(3) Whittall, I. R.; McDonagh, A. M.; Humphrey, M. G.; Samoc, M. *Adv. Organomet. Chem.* **1998**, *42*, 291.
(4) Whittall, I. R.; McDonagh, A. M.; Humphrey, M. G.; Samoc, M. *Adv. Organomet. Chem.* **1999**, *43*, 349.
(5) Heck, J.; Dabek, S.; Meyer-Friedrichsen, T.; Wong, H. *Coord. Chem. Rev.* **1999**, *190*−*192*, 1217.
(6) Morrall, J.; Dalton, G.; Humphrey, M. G.; Samoc, M. *Adv. Organomet. Chem.* **2007**, *55*, 61.
(7) Cheng, L.-T.; Tam, W.; Stevenson, S. H.; Meredith, G. R.; Rikken, G.; Marder, S. R. *J. Phys. Chem.* **1991**, *95*, 10631.

large cubic NLO coefficients.[8] In proceeding to the organometallic realm, the substitution of organic donor groups by ligated metal centers increases molecular design flexibility (the metal, co-ligands, and coordination geometry can all potentially be varied); this often results in quadratic and/or cubic NLO response enhancement and in some instances permits NLO switching by oxidation/reduction at the metal.[9−18] The most heavily studied organometallic complexes in nonlinear optics thus far have been metallocenyl[19−62] or metal alkynyl complexes.[63−66] We have reported extensive studies developing structure−quadratic NLO activity relationships for dipolar metal alkynyl complexes[67−78] and structure−cubic NLO trends,[12,14,15,68,72,79−91] but almost all complexes incorporate π-bridge units containing

(8) Nalwa H. S. In *Nonlinear Optics of Organic Molecules and Polymers*; Nalwa, H. S., Miyata, S., Ed.; CRC Press: Boca Raton, 1997.
(9) Coe, B. J. *Chem.—Eur. J.* **1999**, *5*, 2464.
(10) Delaire, J. A.; Nakatani, K. *Chem. Rev.* **2000**, *100*, 1817.
(11) Weyland, T.; Ledoux, I.; Brasselet, S.; Zyss, J.; Lapinte, C. *Organometallics* **2000**, *19*, 5235.
(12) Cifuentes, M. P.; Powell, C. E.; Humphrey, M. G.; Heath, G. A.; Samoc, M.; Luther-Davies, B. *J. Phys. Chem. A* **2001**, *105*, 9625.
(13) Malaun, M.; Reeves, Z. R.; Paul, R. L.; Jeffery, J. C.; McCleverty, J. A.; Ward, M. D.; Asselberghs, I.; Clays, K.; Persoons, A. *Chem. Commun.* **2001**, 49.
(14) Powell, C. E.; Cifuentes, M. P.; Morrall, J. P. L.; Stranger, R.; Humphrey, M. G.; Samoc, M.; Luther-Davies, B.; Heath, G. A. *J. Am. Chem. Soc.* **2003**, *125*, 602.
(15) Powell, C. E.; Humphrey, M. G.; Cifuentes, M. P.; Morrall, J. P.; Samoc, M.; Luther-Davies, B. *J. Phys. Chem. A* **2003**, *107*, 11264.
(16) Asselberghs, I.; Clays, K.; Persoons, A.; McDonagh, A. M.; Ward, M. D.; McCleverty, J. *Chem. Phys. Lett.* **2003**, *368*, 408.
(17) Paul, F.; Costuas, K.; Ledoux, I.; Deveau, S.; Zyss, J.; Halet, J.-F.; Lapinte, C. *Organometallics* **2002**, *21*, 5229.
(18) Samoc, M.; Gauthier, N.; Cifuentes, M. P.; Paul, F.; Lapinte, C.; Humphrey, M. G. *Angew. Chem., Int. Ed.* **2006**, *45*, 7536.
(19) *Materials for Nonlinear Optics, Chemical Perspectives*; Marder, S. R., Sohn, J. E., Stucky, G. D., Eds.; American Chemical Society: Washington, D.C., 1991.
(20) Sharma, H. K.; Pannell, K. H.; Ledoux, I.; Zyss, J.; Ceccanti, A.; Zanello, P. *Organometallics* **2000**, *19*, 770.
(21) Calabrese, J. C.; Cheng, L. T.; Green, J. C.; Marder, S. R.; Tam, W. *J. Am. Chem. Soc.* **1991**, *113*, 7227.
(22) Cheng, L. T.; Tam, W.; Meredith, G. R. *Mol. Cryst. Liq. Cryst.* **1990**, *189*, 137.
(23) Pedersen, B.; Wagner, G.; Herrmann, R.; Scherer, W.; Meerholz, K.; Schmalzlin, E.; Brauchle, C. *J. Organomet. Chem.* **1999**, *590*, 129.
(24) Pal, S. K.; Krishnan, A.; Das, P. K.; Samuelson, A. G. *J. Organomet. Chem.* **2000**, *604*, 248.
(25) Marder, S. R.; Beratan, D. N.; Tiemann, B. G.; Cheng, L.-T.; Tam, W. In *Organic Materials for Nonlinear Optics II*; Hann, R. A., Bloor, D., Eds.; Royal Society of Chemistry: London, U.K., 1991.
(26) Balavoine, G. G. A.; Daran, J. C.; Iftime, G.; Lacroix, P. G.; Manoury, E.; Delaire, J. A.; Maltey-Fanton, I.; Nakatani, K.; Di Bella, S. *Organometallics* **1999**, *18*, 21.
(27) Cheng, L.-T. In *Organic Molecules for Nonlinear Optics and Photonics*; Messier, J., Kajzar, F., Prasad, P., Eds.; Springer: Berlin, 1991; p 121.
(28) Tiemann, B. G.; Marder, S. R.; Perry, J. W.; Cheng, L.-T. *Chem. Mater.* **1990**, *2*, 690.
(29) Arbez-Gindre, C.; Steele, B. R.; Heropoulos, G. A.; Screttas, C. G.; Communal, J.-E.; Blau, W.; Ledoux-Rak, I. *J. Organomet. Chem.* **2005**, *690*, 1620.
(30) Mata, J.; Uriel, S.; Peris, E.; Llusar, R.; Houbrechts, S.; Persoons, A. *J. Organomet. Chem.* **1998**, *562*, 197.
(31) Mata, J. A.; Peris, E.; Asselberghs, I.; Van Boxel, R.; Persoons, A. *New J. Chem.* **2001**, *25*, 299.
(32) Mata, J. A.; Peris, E.; Asselberghs, I.; Van Boxel, R.; Persoons, A. *New J. Chem.* **2001**, *25*, 1043.
(33) Bourgault, M.; Baum, K.; Le Bozec, H.; Pucetti, G.; Ledoux, I.; Zyss, J. *New J. Chem.* **1998**, *22*, 517.
(34) Krishnan, A.; Pal, S. K.; Nandakumar, P.; Samuelson, A. G.; Das, P. K. *Chem. Phys.* **2001**, *265*, 313.
(35) Lee, I. S.; Lee, S. S.; Chung, Y. K.; Kim, D.; Song, N. W. *Inorg. Chim. Acta* **1998**, *279*, 243.
(36) Malaun, M.; Kowallick, R.; McDonagh, A. M.; Marcaccio, M.; Paul, R. L.; Asselberghs, I.; Clays, K.; Persoons, A.; Bildstein, B.; Fiorini, C.; Nunzi, J. M.; Ward, M. D.; McCleverty, J. A. *J. Chem. Soc., Dalton Trans.* **2001**, 3025.
(37) Yuan, Z.; Taylor, N. J.; Sun, Y.; Marder, T. B. *J. Organomet. Chem.* **1993**, *449*, 27.
(38) Doisneau, G.; Balavoine, G.; Fillebeenkhan, T.; Clinet, J. C.; Delaire, J.; Ledoux, I.; Loucif, R.; Puccetti, G. *J. Organomet. Chem.* **1991**, *421*, 299.
(39) Loucif-Saibi, R.; Delaire, J. A.; Bonazzola, L.; Doisneau, G.; Balavoine, G.; Fillebeenkhan, T.; Ledoux, I.; Puccetti, G. *Chem. Phys.* **1992**, *167*, 369.
(40) Ledoux, I. *Synth. Met.* **1993**, *54*, 123.
(41) Behrens, U.; Brussaard, H.; Hagenau, U.; Heck, J.; Hendrickx, E.; Koernich, J.; van der Linden, J. G. M.; Persoons, A.; Spek, A. L. *Chem.—Eur. J.* **1996**, *2*, 98.
(42) Hagenau, U.; Heck, J.; Hendrickx, E.; Persoons, A.; Schuld, T.; Wong, H. *Inorg. Chem.* **1996**, *35*, 7863.
(43) Malaun, M.; Reeves, Z. R.; Paul, R. L.; Jeffery, J. C.; McCleverty, J. A.; Ward, M. D.; Asselberghs, I.; Clays, K.; Persoons, A. E. *Chem. Commun.* **2001**, 49.
(44) Lee, I. S.; Choi, D. S.; Shin, D. M.; Chung, Y. K.; Choi, C. H. *Organometallics* **2004**, *23*, 1875.
(45) Heck, J.; Dabek, S.; Meyer-Friedrichsen, T.; Wong, H. *Coord. Chem. Rev.* **1999**, *192*, 1217.
(46) Wong, H.; Meyer-Friedrichsen, T.; Farrell, T.; Mecker, C.; Heck, J. *Eur. J. Inorg. Chem.* **2000**, 631.
(47) Blanchard-Desce, M.; Runser, C.; Fort, A.; Barzoukas, M.; Lehn, J. M.; Bloy, V.; Alain, V. *Chem. Phys.* **1995**, *199*, 253.
(48) Moore, A. J.; Chesney, A.; Bryce, M. R.; Batsanov, A. S.; Kelly, J. F.; Howard, J. A. K.; Perepichka, I. F.; Perepichka, D. F.; Meshulam, G.; Berkovuc, G.; Kotler, Z.; Mazor, R.; Khodorkovsky, V. *Eur. J. Org. Chem.* **2001**, *14*, 2671.
(49) Klys, A.; Zakrzewski, J.; Nakatani, K.; Delaire, J. A. *Inorg. Chem. Commun.* **2001**, *4*, 205.
(50) Winter, C. S.; Oliver, S. N.; Rush, J. D. *Opt. Commun.* **1988**, *69*, 45.
(51) Myers, L. K.; Langhoff, C.; Thompson, M. E. *J. Am. Chem. Soc.* **1992**, *114*, 7560.
(52) Li, G.; Song, Y.; Hou, H.; Li, L.; Fan, Y.; Zhu, Y.; Meng, X.; Mi, L. *Inorg. Chem.* **2003**, *42*, 913.
(53) Ghosal, S.; Samoc, M.; Prasad, P. N.; Tufariello, J. J. *J. Phys. Chem.* **1990**, *94*, 2847.
(54) Winter, C. S.; Oliver, S. N.; Rush, J. D. In *Organic Materials for Nonlinear Optics*; Hann, R. A., Bloor, D., Eds.; Royal Society of Chemsitry: London, U.K., 1989; p 232.
(55) Winter, C. S.; Oliver, S. N.; Rush, J. D. In *Nonlinear Optical Effects in Organic Polymers*; Messier, J., Kajzar, F., Prasad, P., Ulrich, D., Eds.; Kluwer: Dordrecht, The Netherlands,1989; p 247.
(56) Calabrese, J. C.; Tam, W. *Chem. Phys. Lett.* **1987**, *133*, 244.
(57) Rojo, G.; Agullo-Lopez, F.; Campo, J. A.; Heras, J. V.; Cano, M. *J. Phys. Chem. B* **1999**, *103*, 11016.
(58) Rojo, G.; Agullo-Lopez, F.; Campo, J. A.; Cano, M.; Lagunas, M. C.; Heras, J. V. *Synth. Met.* **2001**, *124*, 201.
(59) Hurst, S. K.; Humphrey, M. G.; Morrall, J. P.; Cifuentes, M. P.; Samoc, M.; Luther-Davies, B.; Heath, G. A.; Willis, A. C. *J. Organomet. Chem.* **2003**, *670*, 56.
(60) Mata, J. A.; Peris, E.; Llusar, R.; Uriel, S.; Cifuentes, M. P.; Humphrey, M. G.; Samoc, M.; Luther-Davies, B. *Eur. J. Inorg. Chem.* **2001**, 2113.
(61) Hou, H.; Li, G.; Song, Y.; Fan, Y.; Zhu, Y.; Zhu, L. *Eur. J. Inorg. Chem.* **2003**, 2325.
(62) Alain, V.; Blanchard-Desce, M.; Chen, C.-T.; Marder, S. R.; Fort, A.; Barzoukas, M. *Synth. Met.* **1996**, *81*, 133.
(63) Marder, T. B.; Lesley, G.; Yuan, Z.; Fyfe, H. B.; Chow, P.; Stringer, G.; Jobe, I. R.; Taylor, N. J.; Williams, I. D.; Kurtz, S. K. In *Materials for Nonlinear Optics, Chemical Perspectives*; Marder, S. R., Sohn, J. E., Stucky, G. D., Eds.; American Chemical Society: Washington D.C., 1991; p 605.
(64) Nguyen, P.; Lesley, G.; Marder, T. B.; Ledoux, I.; Zyss, J. *Chem. Mater.* **1997**, *9*, 406.
(65) Powell, C. E.; Humphrey, M. G. *Coord. Chem. Rev.* **2004**, *248*, 725.
(66) Cifuentes, M. P.; Humphrey, M. G. *J. Organomet. Chem.* **2004**, *689*, 3968.
(67) Cifuentes, M. P.; Humphrey, M. G.; Morrall, J. P.; Samoc, A.; Paul, F.; Lapinte, C.; Roisnel, T. *Organometallics* **2005**, *24*, 4280.
(68) Hurst, S.; Cifuentes, M. P.; Morrall, J. P. L.; Lucas, N. T.; Whittall, I. R.; Humphrey, M. G.; Asselberghs, I.; Persoons, A.; Samoc, M.; Luther-Davies, B.; Willis, A. C. *Organometallics* **2001**, *20*, 4664.
(69) Whittall, I. R.; Humphrey, M. G.; Persoons, A.; Houbrechts, S. *Organometallics* **1996**, *15*, 1935.

one or two phenyl rings coupled together in various ways; our only study examining π-bridge lengthening, in proceeding from *trans*-[Ru(4-C≡$CC_6H_4NO_2$)Cl(dppm)$_2$] to *trans*-[Ru(4,4′-C≡CC_6H_4C≡$CC_6H_4NO_2$)Cl(dppm)$_2$] and then *trans*-[Ru(4,4′,4″-C≡CC_6H_4C≡CC_6H_4C≡$CC_6H_4NO_2$)Cl(dppm)$_2$], resulted in a nonlinear increase in quadratic nonlinearity as measured by hyper-Rayleigh scattering (HRS) at 1064 nm [β_{1064}: 767 to 833 to 1379; β_0: 129 to 161 to 365 (10^{-30} esu)].[68] [We have very recently prepared and assessed further examples with π-bridges containing three phenyl rings linked by a variety of yne and *E*-ene groups and again noted an increase in quadratic nonlinearity.[1,92]] Unfortunately, attempts to extend the oligo(phenyleneethynylene) series to the tetra(phenyleneethynylene)-containing example resulted in an alkynyl complex with minimal solubility, which hampered reaction and complex characterization and rendered solution NLO studies impossible. We report herein several new oligo(phenyleneethynylene)-containing alkynes incorporating solubilizing substituents, the corresponding ruthenium alkynyl complex derivatives, assessment of the impact of π-bridge lengthening on electrochemical and linear optical properties, theoretical studies using time-dependent density functional theory (TD-DFT) directed at rationalizing our experimental observations, quadratic nonlinear optical properties from hyper-Rayleigh scattering studies at two wavelengths, and wide-spectral-range wavelength-dependence studies of the cubic nonlinear optical properties of selected complexes from Z-scan studies; these studies demonstrate that electrochemical and optical properties in this system converge at the tri(phenyleneethynylene) π-bridge length.

Experimental Section

Materials. All reactions were performed under a nitrogen atmosphere with the use of Schlenk techniques unless otherwise stated. Tetrahydrofuran (THF) was dried by distilling over sodium/benzophenone; all other solvents were used as received. Petrol is a fraction of boiling range 60−80 °C. Chromatography was performed on silica gel or ungraded basic alumina. Ethynyltrimethylsilane (Wacker), *tert*-butyllithium (concentration determined prior to reaction by titration against diphenylacetic acid), 1,2-diiodoethane, 4-bromo-1-iodobenzene, bromine, iodine, sodium hexafluorophosphate, tetra-*n*-butylammonium fluoride, copper(I) iodide, sodium sulfite, magnesium sulfate, sodium acetate, sodium bicarbonate, potassium iodate, $PdCl_2(PPh_3)_2$, and $Pd(PPh_3)_4$ (Aldrich) were used as received. The following were prepared by literature procedures: 1,4-diethoxybenzene,[93] 1,4-dibromo-2,5-diethoxybenzene,[94] 4-Me_3SiC≡CC_6H_4I, 4-HC≡$CC_6H_4NO_2$,[95] 4-HC≡CC_6H_4C≡$CSiPr^i_3$,[96] 4,4′-IC_6H_4C≡CC_6H_4C≡$CSiPr^i_3$,[97] *cis*-[$RuCl_2$(dppe)$_2$], *cis*-[$RuCl_2$(dppm)$_2$],[98] *trans*-[Ru(4-C≡CC_6H_4-NO_2)Cl(dppe)$_2$] (**25**),[99] *trans*-[Ru(4,4′-C≡CC_6H_4C≡$CC_6H_4NO_2$)-Cl(dppe)$_2$] (**26**), *trans*-[Ru(4,4′,4″-C≡CC_6H_4C≡CC_6H_4C≡CC_6H_4-NO_2)Cl(dppe)$_2$] (**27**),[1] *trans*-[Ru(4-C≡$CC_6H_4NO_2$)Cl(dppm)$_2$] (**28**),[100] *trans*-[Ru(4,4′-C≡CC_6H_4C≡$CC_6H_4NO_2$)Cl(dppm)$_2$] (**29**), *trans*-[Ru(4,4′,4″-C≡CC_6H_4C≡CC_6H_4C≡$CC_6H_4NO_2$)Cl(dppm)$_2$] (**30**).[68] The syntheses of **1**−**18** are given in the Supporting Information.

Methods and Instrumentation. Microanalyses were carried out at the Australian National University. UV−vis spectra of solutions in 1 cm quartz cells were recorded as dichloromethane solutions using a Cary 5 spectrophotometer; bands are reported in the form frequency (cm^{-1}) [extinction coefficient (10^4 M^{-1} cm^{-1})]. Infrared spectra were recorded as solutions in dichloromethane or as KBr disks using a Perkin-Elmer System 2000 FT-IR; data are reported in cm^{-1}. ^1H (300 MHz), ^{13}C (75 MHz), and ^{31}P NMR (121 MHz) spectra were recorded using a Varian Gemini-300 FT NMR spectrometer and are referenced to residual chloroform (7.26 ppm), $CDCl_3$ (77.0 ppm), or external H_3PO_4 (0.0 ppm), respectively; atom

(70) Whittall, I. R.; Humphrey, M. G.; Houbrechts, S.; Persoons, A.; Hockless, D. C. R. *Organometallics* **1996**, *15*, 5738.
(71) McDonagh, A. M.; Whittall, I. R.; Humphrey, M. G.; Hockless, D. C. R.; Skelton, B. W.; White, A. H. *J. Organomet. Chem.* **1996**, *523*, 33.
(72) Whittall, I. R.; Cifuentes, M. P.; Humphrey, M. G.; Luther-Davies, B.; Samoc, M.; Houbrechts, S.; Persoons, A.; Heath, G. A.; Hockless, D. C. R. *J. Organomet. Chem.* **1997**, *549*, 127.
(73) Naulty, R. H.; McDonagh, A. M.; Whittall, I. R.; Cifuentes, M. P.; Humphrey, M. G.; Houbrechts, S.; Maes, J.; Persoons, A.; Heath, G. A.; Hockless, D. C. R. *J. Organomet. Chem.* **1998**, *563*, 137.
(74) McDonagh, A. M.; Cifuentes, M. P.; Lucas, N. T.; Humphrey, M. G.; Houbrechts, S.; Persoons, A. *J. Organomet. Chem.* **2000**, *605*, 193.
(75) Whittall, I. R.; Cifuentes, M. P.; Humphrey, M. G.; Luther-Davies, B.; Samoc, M.; Houbrechts, S.; Persoons, A.; Heath, G. A.; Bogsanyi, D. *Organometallics* **1997**, *16*, 2631.
(76) Whittall, I. R.; Humphrey, M. G.; Hockless, D. C. R.; Skelton, B. W.; White, A. H. *Organometallics* **1995**, *14*, 3970.
(77) McDonagh, A. M.; Whittall, I. R.; Humphrey, M. G.; Skelton, B. W.; White, A. H. *J. Organomet. Chem.* **1996**, *519*, 229.
(78) Naulty, R. H.; Cifuentes, M. P.; Humphrey, M. G.; Houbrechts, S.; Boutton, C.; Persoons, A.; Heath, G. A.; Hockless, D. C. R.; Luther-Davies, B.; Samoc, M. *J. Chem. Soc., Dalton Trans.* **1997**, 4167.
(79) Whittall, I. R.; Humphrey, M. G.; Samoc, M.; Luther-Davies, B. *Angew. Chem., Int. Ed. Engl.* **1997**, *36*, 370.
(80) McDonagh, A. M.; Humphrey, M. G.; Samoc, M.; Luther-Davies, B.; Houbrechts, S.; Wada, T.; Sasabe, H.; Persoons, A. *J. Am. Chem. Soc.* **1999**, *121*, 1405.
(81) McDonagh, A. M.; Humphrey, M. G.; Samoc, M.; Luther-Davies, B. *Organometallics* **1999**, *18*, 5195.
(82) Hurst, S.; Lucas, N. T.; Cifuentes, M. P.; Humphrey, M. G.; Samoc, M.; Luther-Davies, B.; Asselberghs, I.; Van Boxel, R.; Persoons, A. *J. Organomet. Chem.* **2001**, *633*, 114.
(83) Hurst, S. K.; Cifuentes, M. P.; McDonagh, A. M.; Humphrey, M. G.; Samoc, M.; Luther-Davies, B.; Asselberghs, I.; Persoons, A. *J. Organomet. Chem.* **2002**, *642*, 259.
(84) Hurst, S. K.; Humphrey, M. G.; Isoshima, T.; Wostyn, K.; Asselberghs, I.; Clays, K.; Persoons, A.; Samoc, M.; Luther-Davies, B. *Organometallics* **2002**, *21*, 2024.
(85) Garcia, M. H.; Robalo, M. P.; Dias, A. R.; Duarte, M. T.; Wenseleers, W.; Aerts, G.; Goovaerts, E.; Cifuentes, M. P.; Hurst, S.; Humphrey, M. G.; Samoc, M.; Luther-Davies, B. *Organometallics* **2002**, *21*, 2107.
(86) Hurst, S. K.; Lucas, N. T.; Humphrey, M. G.; Isoshima, T.; Wostyn, K.; Asselberghs, I.; Clays, K.; Persoons, A.; Samoc, M.; Luther-Davies, B. *Inorg. Chim. Acta* **2003**, *350*, 62.
(87) Hurst, S. K.; Humphrey, M. G.; Morrall, J. P.; Cifuentes, M. P.; Samoc, A.; Luther-Davies, B.; Willis, A. C. *J. Organomet. Chem.* **2003**, *670*, 56.
(88) Cifuentes, M. P.; Powell, C. E.; Morrall, J. P.; McDonagh, A. M.; Lucas, N. T.; Humphrey, M. G.; Samoc, M.; Houbrechts, S.; Asselberghs, I.; Clays, K.; Persoons, A.; Isoshima, T. *J. Am. Chem. Soc.* **2006**, *126*, 10819.
(89) Powell, C. E.; Cifuentes, M. P.; Humphrey, M. G.; Willis, A. C.; Morrall, J. P.; Samoc, M. *Polyhedron* **2007**, *26*, 284.
(90) Samoc, M.; Morrall, J. P.; Dalton, G. T.; Cifuentes, M. P.; Humphrey, M. G. *Angew. Chem., Int. Ed.* **2007**, *46*, 731.
(91) Vicente, J.; Chicote, M. T.; Abrisqueta, M. D.; Ramîrez de Arellano, M. C.; Jones, P. G.; Humphrey, M. G.; Cifuentes, M. P.; Samoc, M.; Luther-Davies, B. *Organometallics* **2000**, *19*, 2968.
(92) Cifuentes, M. P.; Humphrey, M. G.; Samoc, M.; Babgi, B.; Dalton, G. T.; Rigamonti, L. *Poly. Prepr.,* in press. Paper no 1288516.f
(93) Yu, B. Z.; Li, M. K.; Lu, M.; Li, H. L. *Appl. Phys. A: Mater. Sci. Process.* **2003**, *76*, 593.
(94) Maruyama, S.; Kawanishi, Y. *J. Mater. Chem.* **2002**, 2245.
(95) Takahashi, S.; Kuroyama, Y.; Sonogashira, K.; Hagihara, N. *Synthesis* **1980**, 627.
(96) Lavastre, O.; Olivier, L.; Dixneuf, P. H.; Sibandhit, S. *Tetrahedron* **1996**, *52*, 5495.
(97) Dalton, G. T.; Cifuentes, M. P.; Watson, L. A.; Petrie, S.; Stranger, R.; Samoc, M.; Humphrey, M. G. *Inorg. Chem.,* in press. DOI: 10.1021/ic900469y.
(98) Chaudret, B.; Commenges, G.; Poilblanc, R. *J. Chem. Soc., Dalton Trans.* **1984**, 1635.
(99) Touchard, D.; Haquette, P.; Guesmi, S.; Pichon, L. L.; Daridor, A.; Toupet, L.; Dixneuf, P. H. *Organometallics* **1997**, *16*, 3640.
(100) McDonagh, A. M.; Cifuentes, M. P.; Whittall, I. R.; Humphrey, M. G.; Samoc, M.; Luther-Davies, B.; Hockless, D. C. R. *J. Organomet. Chem.* **1996**, *526*, 99.

labeling follows the numbering scheme in Chart S1. Electrospray ionization mass spectra (ESI-MS) were recorded using a Micromass/Water's LC-ZMD single quadrupole liquid chromatograph MS, high-resolution (HR) ESI mass spectra were carried out utilizing a Bruker Apex 4.7T FTICR-MS instrument, and electron impact mass spectra (EI MS) were recorded using a VG Quattro II triple quadrupole MS; all mass spectrometry peaks are reported as m/z (assignment, relative intensity). Cyclic voltammetry measurements were recorded using a MacLab 400 interface and MacLab potentiostat from ADInstruments. The supporting electrolyte was 0.1 M $(NBu^n_4)PF_6$ in distilled, deoxygenated CH_2Cl_2. Solutions containing ca. 1×10^{-3} M complex were maintained under argon. Measurements were carried out at room temperature using Pt disk working, Pt wire auxiliary, and Ag/AgCl reference electrodes, such that the ferrocene/ferrocenium redox couple was located at 0.56 V (peak separation ca. 0.09 V). Scan rates were typically 100 mV s^{-1}.

Synthesis of *trans*-[Ru{4,4′-C≡CC$_6$H$_2$[2,5-(OEt)$_2$]C≡CC$_6$H$_4$NO$_2$}Cl(dppm)$_2$] (19). *cis*-[$RuCl_2$(dppm)$_2$] (132 mg, 0.14 mmol) and $NaPF_6$ (31.3 mg, 0.17 mmol) were added to a solution of **5** (47.1 mg, 0.14 mmol) in CH_2Cl_2 (30 mL). The yellow mixture was stirred at room temperature overnight. NEt_3 (1 mL) was added and the red mixture stirred at room temperature for 6 h. The reaction mixture was purified by passing through a short pad of alumina, eluting with CH_2Cl_2/petrol/NEt_3 (10:10:1). Reduction in volume of the solvent on a rotary evaporator afforded **19** as a dark red powder (120 mg, 69%). ESI-MS: 1240 ($[M]^+$, 100), 1205 ($[M - Cl]^+$, 10). Anal. Calcd for $C_{70}H_{60}ClNO_4P_4Ru \cdot 0.25CH_2Cl_2$: C, 66.92; H, 4.84; N, 1.11. Found: C, 66.95; H, 5.11; N, 1.25. UV−vis: 19 600 [1.8], 26 500 [2.2], 30 400 [1.9]. IR (CH_2Cl_2): 2200, 2064 (C≡C). ^{1}H NMR: δ 1.25, 1.41 (2 t, 6H, J_{HH} = 7 Hz, $2CH_3$), 3.67, 3.82 (2 q, 4H, J_{HH} = 7 Hz, $2CH_2$), 4.80, 5.32 (2 m, 4H, $2PCH_2$), 5.19, 6.77 (2 s, 2H, H_{16}, H_{19}), 5.28 (s, 0.5H, CH_2Cl_2), 6.99−7.60 (m, 44H, H_{24}, Ph), 8.20 (d, J_{HH} = 8 Hz, 2H, H_{25}). ^{13}C NMR: δ 15.1, 15.2 (CH_3), 47.6 (PCH_2), 63.7, 64.4 (CH_2), 91.6, 94.2 (C_{21}, C_{22}), 104.2, 110.4 (C_{15}, C_{18}), 114.1, 117.4 (C_{16}, C_{19}), 123.1 (C_{23}), 123.6 (C_{25}), 127.5 (Ph), 129.0 (d, J_{CP} = 36 Hz, Ph), 131.6 (C_{24}), 133.5 (d, J_{CP} = 38 Hz, Ph), 146.2 (C_{26}), 152.4, 153.7 (C_{17}, C_{20}), C_{13}, C_{14} not observed. ^{31}P NMR: δ −4.7. The syntheses of **20**−**24** are similar and are given in the Supporting Information.

X-ray Structural Study of *trans*-[Ru{4,4′-C≡CC$_6$H$_2$[2,5-(OEt)$_2$]-C≡CC$_6$H$_4$NO$_2$}Cl(dppm)$_2$] (19). A crystal suitable for the structural study was grown by slow diffusion of methanol into a dichloromethane solution of **19** at −20 °C. A unique diffractometer data set was collected on a Nonius Kappa CCD diffractometer using the ω scan technique (graphite-monochromated Mo Kα radiation, 0.71073 Å). The unit cell parameters were obtained by least-squares refinement[101] of 13 727 reflections with $2.6° \le \theta \le 27.5°$ at 200 K. An analytical absorption correction was applied, using numerical methods,[102] implemented from MAXUS,[103] and equivalent reflections were merged. The structure was solved by direct methods, expanded using Fourier techniques,[104] and refined using the CRYSTALS software package.[105,106] One of the phenyl rings attached to a dppm moiety was found to be disordered, and so each atom was split. The total site occupancies were set to be one for each set of split atoms. All other non-hydrogen atoms were refined anisotropically. Hydrogen atoms were included in the refinement at idealized positions, riding on the atoms to which they are bonded, and their positions were frequently recalculated. Conventional residuals R and R_w on $|F|$ were 4.3% and 15.2%, respectively; a Chebyshev weighting function was employed. The largest peaks in the final difference electron density map are located near the Ru atom. Molecular graphics were displayed using the PLATON software.[107]

Crystal/Refinement Data: $C_{70}H_{60}ClNO_4P_4Ru$, M = 1239.67, monoclinic, $P2_1/c$, a = 22.2245(2) Å, b = 12.7995(1) Å, c = 23.5634(2) Å, β = 116.4624(5)°, V = 6000.62(9) Å^3. D_c (Z = 4) = 1.327 g cm^{-3}. μ_{Mo} = 0.46 mm^{-1}; specimen: 0.40 × 0.25 × 0.24 mm; $T_{min/max}$ = 0.857/0.916. $2\theta_{max}$ = 55°; N_{total} = 125 417 (CCD diffractometer, monochromatic Mo Kα radiation, λ = 0.71073 Å; T 200 K) merging to 13 727 unique (R_{int} = 0.044), N_o = 3517 ($I \ge 3\sigma(I)$) refining to R = 0.0425, R_w = 0.152.

Theoretical Studies. Calculations were performed using the Amsterdam Density Functional (ADF) package ADF2006.01,[108] developed by Baerends et al.[109,110] These calculations were undertaken to characterize the lowest frequency allowed single-photon transitions of a set of model compounds containing the oligo(phenyleneethynylene) bridges of compounds **19** to **24**. These models were of the form [Ru]$(C_2C_6H_4)_iC_2C_6H_4NO_2$, where [Ru] = *trans*-$RuCl(PH_2CH_2PH_2)_2$ and i = 1−4. In the discussion that follows, the models are denoted as **19M** (i = 1), **20M** (i = 2), **23M** (i = 3), and **24M** (i = 4) to indicate the laboratory compounds of which they are structural homologues. Note that, for reasons of computational expediency, the solubilizing ethoxy substituents of the laboratory compounds have been omitted in our model calculations. The presence or absence of alkoxy substituents on the phenylene rings has been found to exert only a minor influence on the intensity and wavelength of major single-photon transitions in a detailed computational study of related compounds.[97] Omission of the ethoxy substituents in this instance allowed the structural symmetry of the models to be constrained to C_{2v} throughout. In all calculations and for all atoms, the Slater-type orbital basis sets used were of triple-ζ-plus-polarization quality (TZP). Electrons in orbitals up to and including 1s {C, N, O}, 2p {P, Cl}, and 4d {Ru} were treated in accordance with the frozen-core approximation. Geometry optimizations employed the gradient algorithm of Versluis and Ziegler.[111] Functionals used in the optimization calculations were the local density approximation (LDA) to the exchange potential,[112] the correlation potential of Vosko, Wilk, and Nusair (VWN),[113] and the nonlocal corrections of Perdew, Burke, and Enzerhof (PBE).[114] Following optimization of the model compounds, time-dependent density functional theory (TD-DFT) calculations were pursued using either PBE or the asymptotically correct functional of van Leeuwen and Baerends (LB94).

HRS Measurements. An injection-seeded Nd:YAG laser (Q-switched Nd:YAG Quanta Ray GCR, 1064 nm, 8 ns pulses, 10 Hz) was focused into a cylindrical cell (7 mL) containing the sample. The intensity of the incident beam was varied by rotation of a half-wave plate placed between crossed polarizers. Part of the laser pulse was sampled by a photodiode to measure the vertically polarized incident light intensity. The frequency-doubled light was collected by an efficient condenser system and detected by a

(101) Otwinowski, Z.; Minor, W. In *Methods in Enzymology*; Carter C. W., Jr., Sweet, R. M., Eds., Academic Press: New York, 1997; Vol. 276, p 307.
(102) Coppens, P. In *Crystallographic Computing*; Ahmed, F. R., Hall, S. R., Huber, C. P., Eds.; Munksgaard: Copenhagen, 1970; p 255.
(103) Mackay, S.; Gilmore, C. J.; Edwards, C.; Tremayne, M.; Stewart, N.; Shankland, K., *maXus Computer Program for the Solution and Refinement of Crystal Structures*; Nonius: The Netherlands, MacScience, Japan, The University of Glasgow, 2000.
(104) Altomare, A.; Cascarano, M.; Giacovazzo, C.; Guagliardi, A.; Burla, M. C.; Polidori, G.; Camalli, M. *J. Appl. Crystallogr.* **1994**, *27*, 425.
(105) Watkin, D. J.; Prout, C. K. *J. Appl. Crystallogr.* **2003**, *36*, 1487.
(106) Watkin, D. J.; Prout, C. K.; Pearce, L. J. *CAMERON*; Chemical Crystallography Laboratory, Oxford University: Oxford.
(107) Spek, A. L. *PLATON−Multipurpose Crystallographic Tool*; Utrecht University: Utrecht, The Netherlands, 2008.
(108) Baerends, E. J.; et al. *Amsterdam Density Functional v.2006.01*; S.C.M., Theoretical Chemistry, Vrije Universiteit: Amsterdam, The Netherlands, http://www.scm.com, 2006.
(109) Fonseca Guerra, C. F.; Snijders, J. G.; te Velde, G.; Baerends, E. J. *Theor. Chem. Acc.* **1998**, *99*, 391.
(110) te Velde, G.; Bickelhaupt, F. M.; Baerends, E. J.; Guerra, C. F.; van Gisbergen, S. J. A.; Snijders, J. G.; Ziegler, T. *J. Comput. Chem.* **2001**, *22*, 931.
(111) Versluis, L.; Ziegler, T. *J. Chem. Phys.* **1988**, *88*, 322.
(112) Parr, R. G.; Yang, W. *Density Functional Theory of Atoms and Molecules*; Oxford University Press: New York, 1989.
(113) Vosko, S. H.; Wilk, L.; Nusair, M. *Can. J. Phys.* **1980**, *58*, 1200.
(114) Perdew, J. P.; Burke, K.; Ernzerhof, M. *Phys. Rev. Lett.* **1996**, *77*, 3865.

photomultiplier. The harmonic scattering and linear scattering were distinguished by appropriate filters; gated integrators were used to obtain intensities of the incident and harmonic scattered light. The absence of a luminescence contribution to the harmonic signal was confirmed by using interference filters at different wavelengths near 532 nm. All measurements were performed in THF using *p*-nitroaniline ($\beta = 21.4 \times 10^{-30}$ esu[115]) as a reference. Solutions were sufficiently dilute that absorption of scattered light was negligible.

For studies at 1.300 μm, a Tsunami-pumped OPAL (model Spectra-Physics) was used. With a high repetition rate of the laser, high-frequency demodulation of fluorescence contributions can be effected, a full description being given in ref 116. All measurements were performed in THF using Disperse Red 1 (DR1, $\beta = 54 \times 10^{-30}$ esu in chloroform) as a reference. Experiments utilized low chromophore concentrations, the linearity of the HRS signal as a function of the chromophore concentration confirming that no significant self-absorption of the SHG signal occurred.

Z-Scan Studies. The compounds were dissolved in dichloromethane at concentrations in the range 0.5−1.2% w/w, and the solutions were placed in 1 mm path length Starna glass cells, stoppered, and sealed with Teflon tape. Due to experimental limitations, only one concentration of each compound was examined. The Z-scans were carried out using a femtosecond laser system composed of a Clark-MXR CPA-2001 regenerative amplifier acting as a 775 nm pump and a Light Conversion TOPAS optical parametric amplifier. The system was operated at a repetition rate of 250 Hz to minimize the influence of thermal effects and photochemical decomposition. The experiments were carried out at a number of wavelengths in the range 530−1500 nm. To obtain the relevant wavelengths, the optical parametric amplifier was tuned appropriately and one of the following modes of output was selected: idler-pump mixing, signal doubling, idler doubling, or the signal. The unwanted components of the TOPAS output were discarded through the use of polarizing optics, color glass filters, and spatial filtering.

The laser beam was attenuated to energies in the μJ/pulse range and directed through a standard Z-scan setup equipped with a beam splitter, allowing one to record open-aperture and closed-aperture Z-scans simultaneously. The beam was focused so as to provide a spot size in the range $w_0 \approx 40-80$ μm, ensuring that the Rayleigh range $z_R = \pi w_0^2/\lambda$ was always larger than the total thickness of the sample (≈3 mm, which includes two glass walls and the solution inside the cell). The cell travel was $z = -40$ to 40 mm, and the data were recorded using three Si or InGaAs photodiodes monitoring the input pulse energy, the open-aperture signal, and the closed-aperture signal, respectively. The outputs were fed into three channels of a boxcar averager, which was GPIB-interfaced with a data collection computer. The shapes of the closed-aperture scans, open-aperture scans, and the curves obtained by dividing a closed-aperture curve by an open-aperture curve were analyzed with the help of a custom fitting program that used equations derived by Sheik-Bahae et al.[117] to calculate the theoretical curves. In this way, the values of the real and imaginary part of the nonlinear phase shift $\Delta\Phi_0$ (corresponding to the refractive and absorptive nonlinearity, respectively) could be obtained. At each wavelength the energy of the laser pulses was adjusted, based on closed-aperture Z-scans obtained for 1 mm cells filled with the solvent alone and/or scans for a 3 mm thick silica glass plate. Typically, we required $\Delta\Phi_0$ for such scans to be about 0.5−1 rad. The nonlinear refractive index of silica, n_2, is well known across a wide wavelength range, so the real part of the nonlinear phase shift can be used to calculate the light intensity. From the comparison of n_2 values for silica compiled by Milam[118] we employed

$$n_{2,\mathrm{silica}}(\bar{\nu}) = 2.82 \times 10^{-16} - 3 \times 10^{-21}\bar{\nu} + 2 \times 10^{-25}\bar{\nu}^2 (\mathrm{cm}^2/\mathrm{W})$$

for the spectral dependence of n_2 for silica, where $\bar{\nu} = 1/\lambda$ is the wavenumber expressed in cm^{-1}. This equation is a good approximation for values of $n_{2,\mathrm{silica}}$ in the range of $\lambda = 500-1500$ nm. Note that most of our previous papers assumed $n_{2,\mathrm{silica}} = 3 \times 10^{-16}$ cm^2/W independent of the wavelength, which is also a reasonably good approximation.

We employed intensities on the order of 100 GW/cm^2. Since our measurements were always uniformly calibrated to the nonlinearity of silica glass, this avoided the need for detailed information of beam geometry and pulse shape.

The real and imaginary parts of the second hyperpolarizability, γ, of the solutes were computed assuming additivity of the nonlinear contributions of the solvent and the solute and the applicability of the Lorentz local field approximation.[119] The values of the two-photon absorption (TPA) cross-section σ_2 were computed from the absorptive part of the nonlinearity determined from the Z-scans. In all cases, errors of the relevant quantities were estimated from the assessed accuracies of the parameters for the fitting of Z-scans for the solutions and the corresponding scans for the solvent.

Results

Synthesis and Characterization of Alkynes. The acetylenes required for the alkynyl complex syntheses were prepared by extensions of established organic synthetic procedures (Schemes 1−6). Monobromination of 1,4-di(ethoxy)benzene using bromine and sodium acetate in acetic acid afforded 1-bromo-2,5-diethoxybenzene (**1**), in a procedure previously applied to afford the 1-bromo-2,5-di(*n*-propoxy)benzene analogue (Scheme 1).[120] Subsequent iodination with iodine/potassium iodate in an acetic acid/carbon tetrachloride mixture afforded 4-bromo-2,5-diethoxy-1-iodobenzene (**2**) in good yield. This facile synthesis of **2** is preferable to the trans-halogenation of 1,4-dibromo-2,5-di(ethoxy)benzene employing *tert*-butyllithium and 1,2-diiodoethane.

Both the bromo and iodo functionalities in **2** are reactive. 4-Ethynyl-1-nitrobenzene and 4-ethynyl-1-(triisopropylsilyl)-ethynylbenzene reacted with **2** under Sonogashira conditions at room temperature to give 2,5-$(EtO)_2$-4-$BrC_6H_2C{\equiv}C$-4-$C_6H_4NO_2$ (**3**) and 4-$Pr^i_3SiC{\equiv}CC_6H_4C{\equiv}CC_6H_2$-2,5-$(OEt)_2$-4-Br (**6**), respectively, in excellent yields (Scheme 2). The former reacted with ethynyltrimethylsilane under Sonogashira conditions to afford 4-$Me_3SiC{\equiv}C$-2,5-$(EtO)_2C_6H_2$-1-$C{\equiv}CC_6H_4$-4-NO_2 (**4**) in fair yield. The diyne **4** was desilylated to afford 4-$HC{\equiv}C$-2,5-$(EtO)_2C_6H_2$-1-$C{\equiv}CC_6H_4$-4-NO_2 (**5**).

Syntheses of tri(phenyleneethynylene)-containing compounds are summarized in Scheme 3. **5** underwent sequential Sonogashira coupling with 4-bromo-1-iodobenzene and then ethynyltrimethylsilane to afford 4-$O_2NC_6H_4C{\equiv}CC_6H_2$-2,5-$(OEt)_2$-4-$C{\equiv}CC_6H_4$-4-$C{\equiv}CSiMe_3$ (**7**), which was desilylated by tetra-*n*-butylammonium fluoride, giving 4-$O_2NC_6H_4C{\equiv}CC_6H_2$-2,5-$(OEt)_2$-4-$C{\equiv}CC_6H_4$-4-$C{\equiv}CH$ (**8**). A similar sequential Sonogashira coupling with 4-Br-2,5-$(EtO)_2C_6H_2$I and then ethynyltrimethylsilane gave 4-$O_2NC_6H_4C{\equiv}CC_6H_2$-2,5-$(OEt)_2$-4-$C{\equiv}CC_6H_2$-2,5-$(OEt)_2$-4-$C{\equiv}CSiMe_3$ (**10**), which was similarly desilylated to

(115) Stähelin, M.; Burland, D. M.; Rice, J. E. *Chem. Phys. Lett.* **1992**, *191*, 245.
(116) Olbrechts, G.; Wostyn, K.; Clays, K.; Persoons, A. *Opt. Lett.* **1999**, 403.
(117) Sheik-Bahae, M.; Said, A. A.; Wei, T.; Hagan, D. J.; van Stryland, E. W. *IEEE J. Quantum Electr.* **1990**, *26*, 760.
(118) Milam, D. *Appl. Opt.* **1998**, *37*, 546.
(119) Samoc, M.; Samoc, A.; Luther-Davies, B.; Humphrey, M. G.; Wong, M.-S. *Opt. Mater.* **2002**, *21*, 485.
(120) Meier, H.; Ickenroth, D.; Stalmach, U.; Koynov, K.; Bahtiar, A.; Bubeck, C. *Eur. J. Org. Chem.* **2001**, 4431.

Scheme 1. Syntheses of **1** and **2**

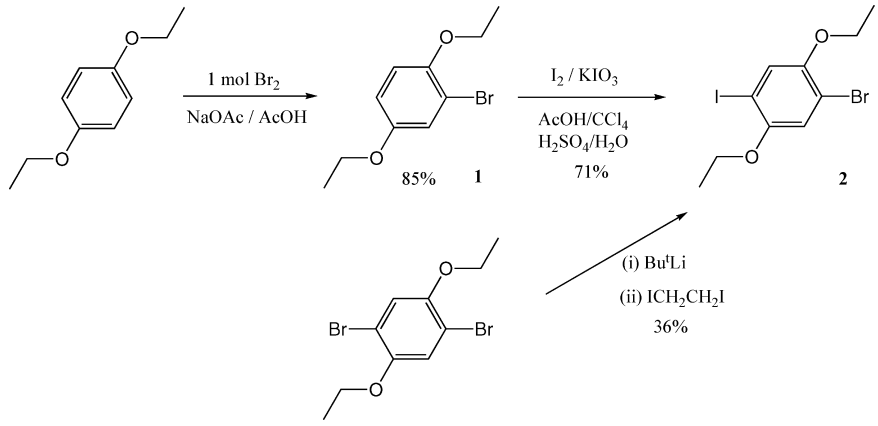

Scheme 2. Syntheses of **3**−**6**

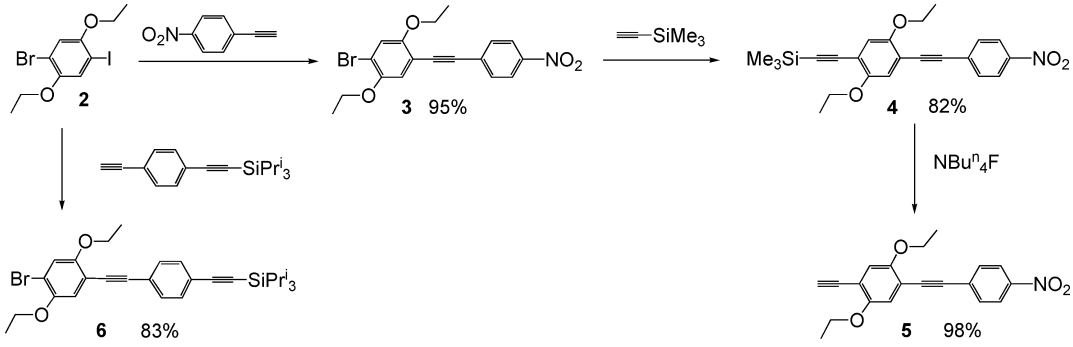

Scheme 3. Syntheses of **7**−**11**

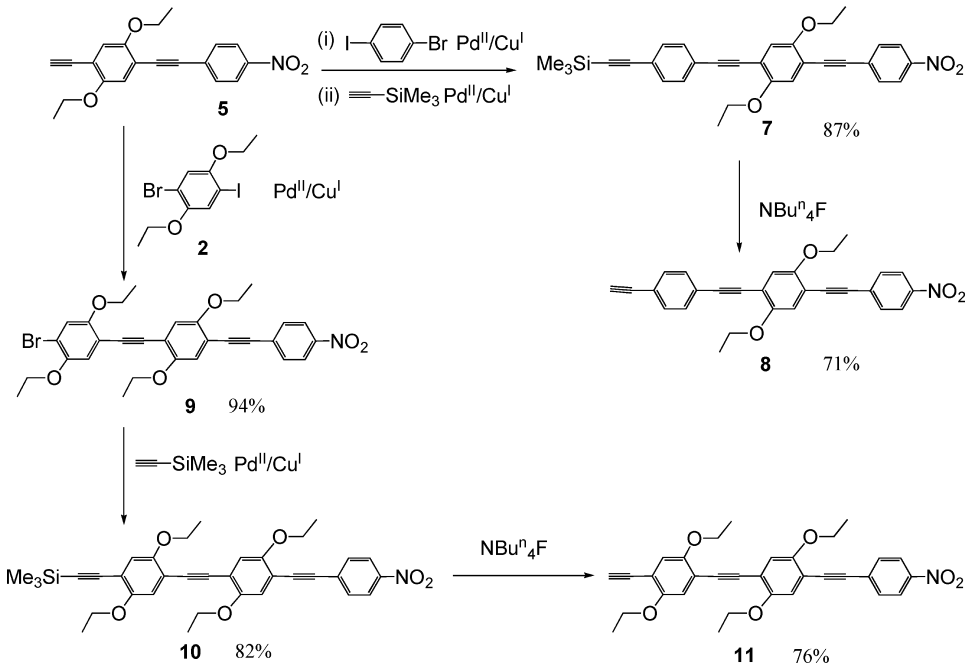

4-$O_2NC_6H_4C{\equiv}CC_6H_2$-2,5-$(OEt)_2$-4-$C{\equiv}CC_6H_2$-2,5-$(OEt)_2$-4-$C{\equiv}CH$ (**11**).

Syntheses of tetra(phenyleneethynylene)-containing compounds in which two rings bear solubilizing groups are summarized in Scheme 4. 4-$Pr^i_3SiC{\equiv}CC_6H_4C{\equiv}CC_6H_2$-2,5-$(OEt)_2$-4-$C{\equiv}CC_6H_2$-2,5-$(OEt)_2$-4-$C{\equiv}CC_6H_4$-4-$NO_2$ (**12**) is available from reaction of **5** with **6** under Sonogashira conditions; **12** was desilylated by tetra-*n*-butylammonium fluoride to give 4-$HC{\equiv}CC_6H_4C{\equiv}CC_6H_2$-2,5-$(OEt)_2$-4-$C{\equiv}CC_6H_2$-2,5-$(OEt)_2$-4-$C{\equiv}CC_6H_4$-4-$NO_2$ (**14**) in quantitative yield. **14** is also accessible from a sequential Sonogashira coupling of **11** with 4-bromo-1-iodobenzene and then ethynyltrimethylsilane, affording 4-$Me_3SiC{\equiv}CC_6H_4C{\equiv}CC_6H_2$-2,5-$(OEt)_2$-4-$C{\equiv}CC_6H_2$-2,5-$(OEt)_2$-4-$C{\equiv}CC_6H_4$-4-$NO_2$ (**13**) and a subsequent desilylation. Syntheses of tetra(phenyleneethynylene)-containing compounds in which one ring bears solubilizing groups are summarized in Scheme

Scheme 4. Syntheses of **12**−**14**

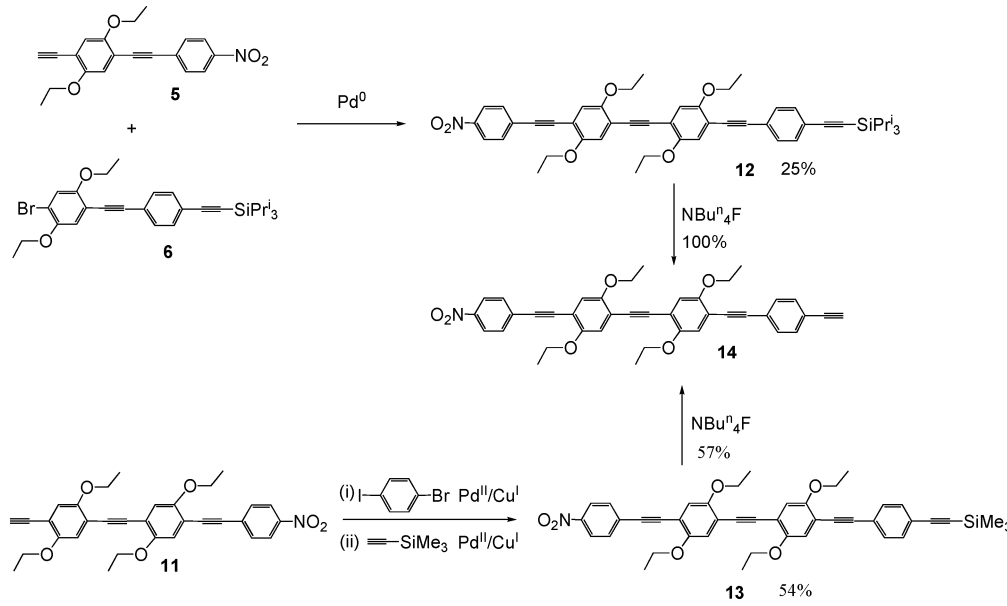

Scheme 5. Syntheses of **15**−**17**

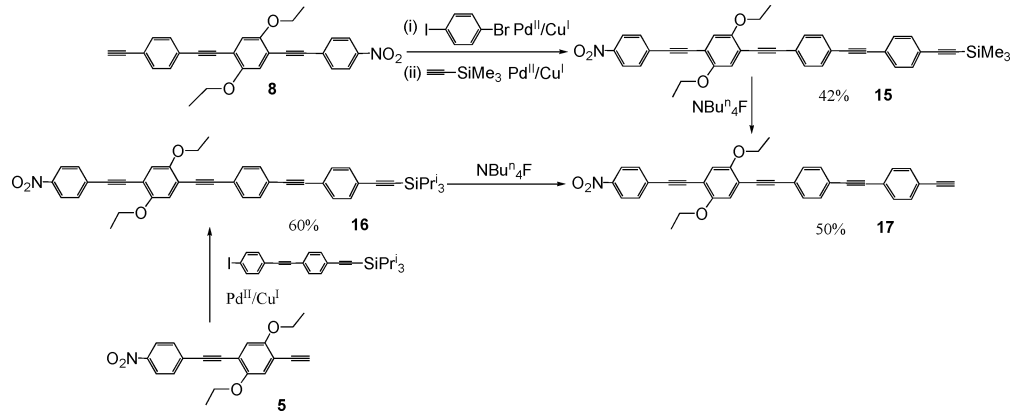

Scheme 6. Synthesis of **18**

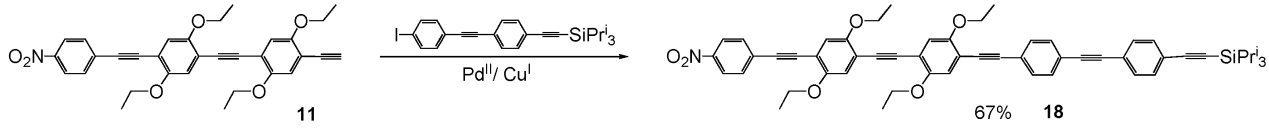

5. Sequential Sonogashira coupling of **8** with 4-bromo-1-iodobenzene and then ethynyltrimethylsilane gave 4-$Me_3SiC{\equiv}CC_6H_4$-1-$C{\equiv}CC_6H_4$-4-$C{\equiv}CC_6H_2$-2,5-$(OEt)_2$-4-$C{\equiv}CC_6H_4$-4-NO_2 (**15**) in a good yield, subsequent desilylation affording 4-$HC{\equiv}CC_6H_4C{\equiv}CC_6H_4$-4-$C{\equiv}CC_6H_2$-2,5-$(OEt)_2$-4-$C{\equiv}CC_6H_4$-4-$NO_2$ (**17**). Alternatively, **5** was coupled to 4-$IC_6H_4C{\equiv}CC_6H_4$-4-$C{\equiv}CSiPr^i_3$ to afford 4-$Pr^i_3SiC{\equiv}CC_6H_4$-1-$C{\equiv}CC_6H_4$-4-$C{\equiv}CC_6H_2$-2,5-$(OEt)_2$-4-$C{\equiv}CC_6H_4$-4-NO_2 (**16**), which was desilylated to give **17** in a better yield. The penta(phenyleneethynylene) 4-$Pr^i_3SiC{\equiv}CC_6H_4$-1-$C{\equiv}CC_6H_4$-4-$C{\equiv}CC_6H_2$-2,5-$(OEt)_2$-4-$C{\equiv}CC_6H_2$-2,5-$(OEt)_2$-4-$C{\equiv}CC_6H_4$-4-NO_2 (**18**) was obtained via Sonogashira coupling of **11** with 4-$IC_6H_4C{\equiv}CC_6H_4$-4-$C{\equiv}CSiPr^i_3$ in a fair yield (Scheme 6).

Synthesis and Characterization of Alkynyl Complexes. The new alkynyl complexes **19**−**24** were prepared using established methodologies (Schemes 7 and 8)[77,99,121−131] and characterized by a combination of IR, ^1H, ^{13}C, and ^{31}P NMR spectroscopies and ESI mass spectrometry. The IR spectra contain characteristic $\nu(C{\equiv}C)$ bands at 2063−2074 cm^{-1} for the metal-bound alkynyl group, with the higher values corresponding to complexes with the longer π-bridges (**22**−**24**). The ^{31}P NMR spectrum of the dppe-containing complex **21** contains one singlet resonance at 49.8 ppm, confirming the *trans*-disposed diphosphine ligands. The spectra of the dppm-containing complexes similarly contain a singlet; the ^{31}P resonance for the complex with ethoxy substituents on the ring adjacent to the metal center (**19**: −4.7 ppm) is somewhat downfield of those of other dppm-containing complexes (−5.5 ppm). Mass spectra contain molecular ions and/or fragment ions corresponding to loss of a chloro ligand.

The identity of **19** was confirmed by a single-crystal X-ray diffraction study. Figure 1 contains an ORTEP plot showing the molecular geometry, together with selected bond lengths

Scheme 7. Syntheses of **19**−**23**

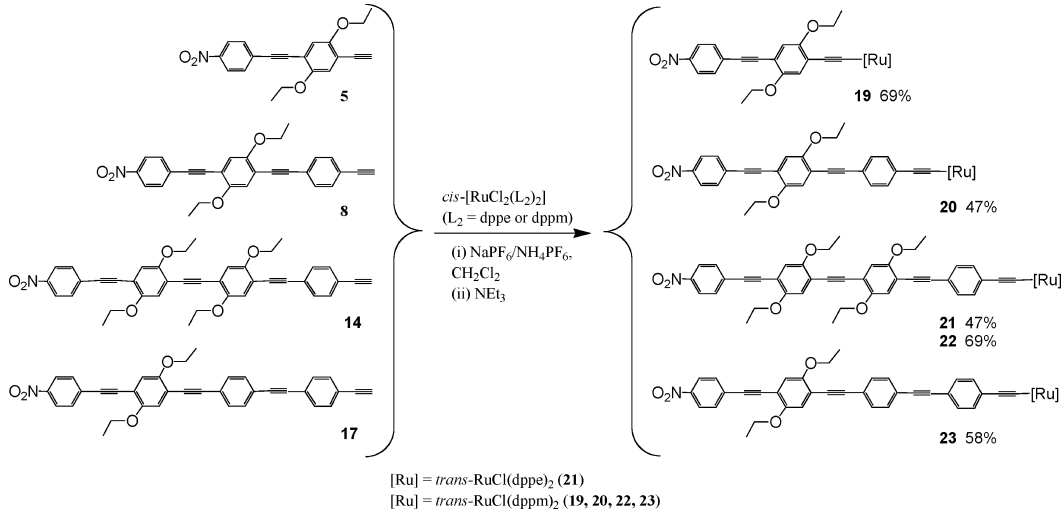

Scheme 8. Synthesis of **24**

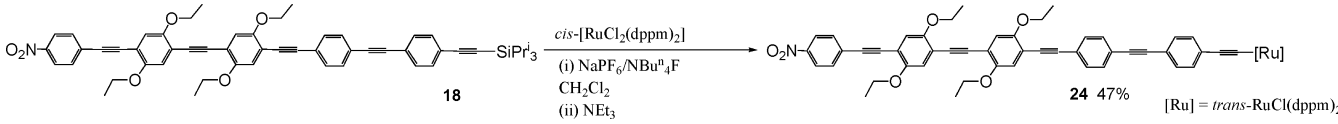

and angles. Bond lengths and angles are similar to those of the structurally characterized analogues *trans*-[Ru(C≡C-4-C_6H_4C≡CC_6H_4-4-X)Cl(dppm)$_2$] (X = H,[68] N═NC_6H_4-4-NO_2[124]), the only notable exception being Cl1−Ru1−Cl 170.33(9)° (**19**), cf. 175.9(2)° (X = H), 175.1(17)° (X = N═NC_6H_4-4-NO_2), a distortion in **19** likely to derive from the need to minimize unfavorable steric interactions between the C4-ethoxy group and the P-phenyl rings. The dihedral angle between the C3/C8 and C11/C16 phenyl planes in **19** (5.7(2)°) is much smaller than those in precedent structural studies (26.75° (X = H), 21.9° (X = N═NC_6H_4-4-NO_2), 33.9° (*trans*-[Ru(C≡C-4-C_6H_4C≡C-4-C_6H_4C≡CPh)$_2$(dmpe)$_2$][132])). Because coplanar phenyl rings in extended π-systems enhance π-delocalization, this structural difference is likely to favorably influence nonlinearity in solid-state materials; however, the centrosymmetric packing in the crystal structure of **19** will result in no bulk second-order susceptibility.

Electrochemical and Linear Optical Studies. Electrochemical properties of ruthenium alkynyl complexes are of significant interest (see ref 92 and references therein). The results of cyclic voltammetric studies of the new ruthenium alkynyl complexes **19**−**24** are collected in Table 1, together with data from related complexes **25**−**30**.

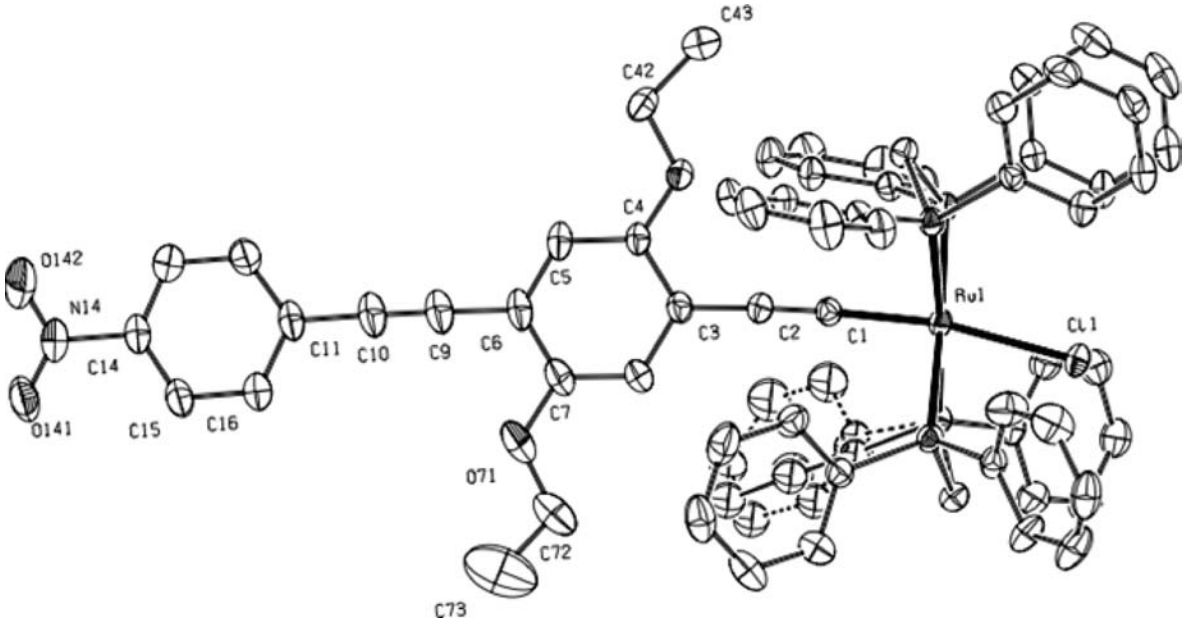

Figure 1. Molecular geometry and atomic labeling scheme for *trans*-[Ru{4,4′-C≡CC_6H_2[2,5-(OEt)$_2$]C≡C$C_6H_4NO_2$}Cl(dppm)$_2$] (**19**). Selected bond lengths (Å) and angles (deg): Ru1−P1 2.3291(8), Ru1−P2 2.3362(8), Ru1−P3 2.3613(8), Ru1−P4 2.3504(8), Ru1−Cl1 2.5176(7), Ru1−C1 1.988(3), C1−C2 1.217(5), C2−C3 1.421(4); P1−Ru1−P2 71.76(3), P3−Ru1−P4 70.87(3), Cl1−Ru1−C1 170.33(9), Ru1−C1−C2 177.2(3), C1−C2−C3 175.8(4).

Table 1. Cyclic Voltammetric Data for Complexes **19**−**30**[a]

complex	E^0_{ox} (V) [i_{pc}/i_{pa}] $Ru^{II/III}$	E^0_{red} (V) [i_{pc}/i_{pa}] $NO_2^{0/-I}$	ref
trans-[Ru(4-C≡$CC_6H_4NO_2$)Cl(dppe)$_2$] (**25**)	0.74 [0.9]	−0.84 [0.8]	68
trans-[Ru(4,4′-C≡CC_6H_4C≡$CC_6H_4NO_2$)Cl(dppe)$_2$] (**26**)	0.60 [1]	−0.94 [0.9]	1
trans-[Ru(4,4′,4″-C≡CC_6H_4C≡CC_6H_4C≡$CC_6H_4NO_2$)Cl(dppe)$_2$] (**27**)	0.58 [1]	−0.91 [0.9]	1
trans-[Ru{4,4′,4″,4‴-C≡CC_6H_4C≡CC_6H_2[2,5-$(OEt)_2$]C≡CC_6H_2[2,5-$(OEt)_2$]C≡$CC_6H_4NO_2$}Cl(dppe)$_2$] (**21**)	0.56 [0.9]	−1.16 [0.9]	this work
trans-[Ru(4-C≡$CC_6H_4NO_2$)Cl(dppm)$_2$] (**28**)	0.72 [1]	−0.81 [0.7],	68
trans-[Ru(4,4′-C≡CC_6H_4C≡$CC_6H_4NO_2$)Cl(dppm)$_2$] (**29**)	0.57 [0.9]	−0.90 [0.7]	68
trans-[Ru{4,4′-C≡CC_6H_2[2,5-$(OEt)_2$]C≡$CC_6H_4NO_2$}Cl(dppm)$_2$] (**19**)	0.50 [1]	−0.91 [0.9]	this work
trans-[Ru(4,4′,4″-C≡CC_6H_4C≡CC_6H_4C≡$CC_6H_4NO_2$)Cl(dppm)$_2$] (**30**)	0.54 [1]	−0.86 [0.9]	68
trans-[Ru{4,4′,4″-C≡CC_6H_4C≡CC_6H_2[2,5-$(OEt)_2$]C≡$CC_6H_4NO_2$}Cl(dppm)$_2$] (**20**)	0.54 [1]	−0.86 [0.9]	this work
trans-[Ru{4,4′,4″,4‴-C≡CC_6H_4C≡CC_6H_2[2,5-$(OEt)_2$]C≡CC_6H_2[2,5-$(OEt)_2$]C≡$CC_6H_4NO_2$}Cl(dppm)$_2$] (**22**)	0.55 [1]	−0.87 [0.9]	this work
trans-[Ru{4,4′,4″,4‴-C≡CC_6H_4C≡CC_6H_4C≡CC_6H_2[2,5-$(OEt)_2$]C≡$CC_6H_4NO_2$}Cl(dppm)$_2$] (**23**)	0.55 [1]	−0.89 [0.9]	this work
trans-[Ru{4,4′,4″,4‴,4⁗-C≡CC_6H_4C≡CC_6H_4C≡CC_6H_2[2,5-$(OEt)_2$]C≡CC_6H_2[2,5-$(OEt)_2$]C≡$CC_6H_4NO_2$}Cl(dppm)$_2$] (**24**)	0.56 [0.9]	−0.90 [0.6]	this work

[a] Conditions: CH_2Cl_2; Pt-wire auxiliary, Pt working, and Ag/AgCl reference electrodes; ferrocene/ferrocenium couple located at 0.56 V.

Table 2. Experimental Linear Optical, Quadratic Nonlinear Optical,[a] and Two-Photon Absorption[b] Response Parameters

complex	λ_{max} (nm) [ϵ, 10^4 M^{-1} cm^{-1}]	β_{1064} (10^{-30} esu)	β_0 (10^{-30} esu)[c]	β_{1300} (10^{-30} esu)	β_0 (10^{-30} esu)[d]	TPA λ_{max} (nm) [$\sigma_{2,max}$, GM][e]	ref
trans-[Ru(4-C≡$CC_6H_4NO_2$)Cl(dppe)$_2$] (**25**)	477 [2.0]	562	88				1
trans-[Ru(4,4′-C≡CC_6H_4C≡$CC_6H_4NO_2$)Cl(dppe)$_2$] (**26**)	468 [1.8]	1240 ± 110	225 ± 20	64 ± 3	27 ± 1		1
trans-[Ru(4,4′,4″-C≡CC_6H_4C≡CC_6H_4C≡$CC_6H_4NO_2$)Cl(dppe)$_2$] (**27**)	429 [2.3]	1327 ± 110	388 ± 32	42 ± 2	21 ± 1		1
trans-[Ru{4,4′,4″,4‴-C≡CC_6H_4C≡CC_6H_2[2,5-$(OEt)_2$]C≡CC_6H_2[2,5-$(OEt)_2$]C≡$CC_6H_4NO_2$}Cl(dppe)$_2$] (**21**)	426 [4.3]	515 ± 50	160 ± 15				this work
trans-[Ru(4-C≡$CC_6H_4NO_2$)Cl(dppm)$_2$] (**28**)	473 [1.8]	767	129	40 ± 6	16 ± 3	940 [135]	73, 1, this work
trans-[Ru(4,4′-C≡CC_6H_4C≡$CC_6H_4NO_2$)Cl(dppm)$_2$] (**29**)	464 [1.4]	833	161	78 ± 4	33 ± 2	890 [567]	68, 1, this work
trans-[Ru{4,4′-C≡CC_6H_2[2,5-$(OEt)_2$]C≡$CC_6H_4NO_2$}Cl(dppm)$_2$] (**19**)	510 [1.8]	570 ± 90	40 ± 6	90 ± 10			this work
trans-[Ru(4,4′,4″-C≡CC_6H_4C≡CC_6H_4C≡$CC_6H_4NO_2$)Cl(dppm)$_2$] (**30**)	439 [2.0]	1379	365				68
trans-[Ru{4,4′,4″-C≡CC_6H_4C≡CC_6H_2[2,5-$(OEt)_2$]C≡$CC_6H_4NO_2$}Cl(dppm)$_2$] (**20**)	459 [2.5]	916 ± 153	400 ± 70	72 ± 12	15 ± 3	890 [1160]	this work
trans-[Ru{4,4′,4″,4‴-C≡CC_6H_4C≡CC_6H_2[2,5-$(OEt)_2$]C≡CC_6H_2[2,5-$(OEt)_2$]C≡$CC_6H_4NO_2$}Cl(dppm)$_2$] (**22**)	424 [3.9]	678 ± 139	208 ± 42	69 ± 5	62 ± 5		this work
trans-[Ru{4,4′,4″,4‴-C≡CC_6H_4C≡CC_6H_4C≡CC_6H_2[2,5-$(OEt)_2$]C≡$CC_6H_4NO_2$}Cl(dppm)$_2$] (**23**)	411 [4.9]	632 ± 103	217 ± 35	108 ± 5	97 ± 5	840 [780]	this work
trans-[Ru{4,4′,4″,4‴,4⁗-C≡CC_6H_4C≡CC_6H_4C≡CC_6H_2[2,5-$(OEt)_2$]C≡CC_6H_2[2,5-$(OEt)_2$]C≡$CC_6H_4NO_2$}Cl(dppm)$_2$] (**24**)	423 [5.6]	580 ± 20	185 ± 10			840 [853]	this work

[a] Conditions: measurements were carried out in THF; all complexes are optically transparent at 1064 and 1300 nm. The β data are ±10% unless specified otherwise. [b] Conditions: measurements were carried out in CH_2Cl_2. [c] Corrected for resonance enhancement at 532 nm using the two-level model with $\beta_0 = \beta[1 - (2\lambda_{max}/1064)^2][1 - (\lambda_{max}/1064)^2]$. [d] Corrected for resonance enhancement at 650 nm using the two-level model with $\beta_0 = \beta[1 - (2\lambda_{max}/1300)^2][1 - (\lambda_{max}/1300)^2]$. [e] The accuracy of the σ_2 data are ±10%.

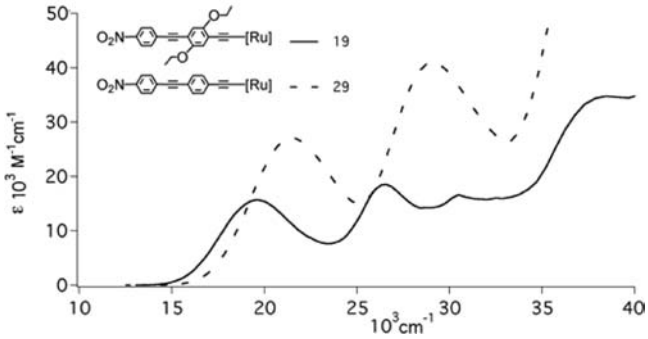

Figure 2. Optical spectra of *trans*-[Ru(4,4′-C≡CC_6H_4C≡$CC_6H_4NO_2$)-$Cl(dppm)_2$] (**29**) and *trans*-[Ru{4,4′-C≡CC_6H_2[2,5-$(OEt)_2$]C≡CC_6H_4-NO_2}$Cl(dppm)_2$] (**19**).

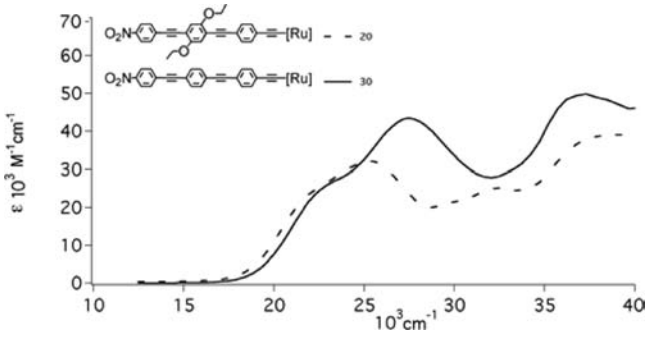

Figure 3. Optical spectra of *trans*-[Ru(4,4′,4″-C≡CC_6H_4C≡CC_6H_4C≡$CC_6H_4NO_2$)$Cl(dppm)_2$] (**30**) and *trans*-[Ru{4,4′,4″-C≡CC_6H_4C≡CC_6H_2[2,5-$(OEt)_2$]C≡$CC_6H_4NO_2$}$Cl(dppm)_2$] (**20**).

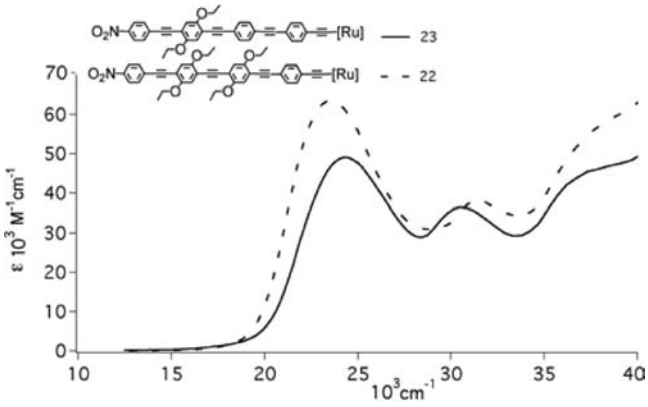

Figure 4. Optical spectra of *trans*-[Ru{4,4′,4″,4‴-C≡CC_6H_4C≡CC_6H_2[2,5-$(OEt)_2$]C≡CC_6H_2[2,5-$(OEt)_2$]C≡$CC_6H_4NO_2$}$Cl(dppm)_2$] (**22**) and *trans*-[Ru{4,4′,4″,4‴-C≡CC_6H_4C≡CC_6H_4C≡CC_6H_2[2,5-$(OEt)_2$]C≡$CC_6H_4NO_2$}$Cl(dppm)_2$] (**23**).

As with other *trans*-bis(bidentate diphosphine)ruthenium monoalkynyl complexes, the cyclic voltammograms of the new complexes contain a reversible or quasi-reversible anodic wave assigned to the $Ru^{II/III}$ oxidation process, in the range 0.50−0.56 V, and a less reversible cathodic wave assigned to the $NO_2^{0/-1}$ reduction process, in the range −0.86 to −1.16 V. These data, together with those of the previously reported complexes **25**−**30**, permit comment on the effect of π-bridge lengthening and solubilizing group incorporation upon metal-localized oxidation potential. For the dppe-containing complexes, OPE increase (proceeding from **25** to **26** to **27** and finally **21**) leads to a progressive decrease in $Ru^{II/III}$ oxidation potential, but this is not clear-cut because of the introduction of ethoxy groups at **21**. The effect of these solubilizing substituents can in principle

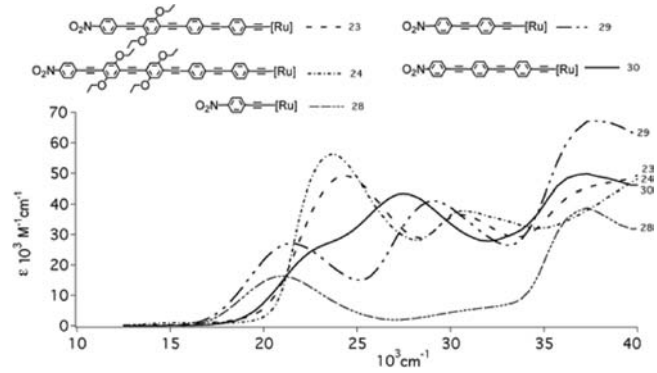

Figure 5. Optical spectra of *trans*-[Ru{4,4′,4″,4‴-C≡CC_6H_4C≡CC_6H_4C≡CC_6H_2[2,5-$(OEt)_2$]C≡$CC_6H_4NO_2$}$Cl(dppm)_2$](**23**),*trans*-[Ru{4,4′,4″,4‴,4⁗-C≡CC_6H_4C≡CC_6H_4C≡CC_6H_2[2,5-$(OEt)_2$]C≡CC_6H_2[2,5-$(OEt)_2$]C≡$CC_6H_4NO_2$}$Cl(dppm)_2$] (**24**), *trans*-[Ru(4-C≡$CC_6H_4NO_2$)-$Cl(dppm)_2$] (**28**), *trans*-[Ru(4,4′-C≡CC_6H_4C≡$CC_6H_4NO_2$)$Cl(dppm)_2$] (**29**), and *trans*-[Ru(4,4′,4″-C≡CC_6H_4C≡CC_6H_4C≡$CC_6H_4NO_2$)$Cl(dppm)_2$] (**30**).

be deconvoluted by examination of the more extensive data available for the dppm-containing complexes. Thus, introduction of solubilizing substituents at the π-bridge phenyl ring adjacent to the metal (proceeding from **29** to **19**) results in a significant increase in the ease of oxidation (ΔE^0_{ox} 0.07 V), whereas solubilizing group introduction more remote from the metal (proceeding from **30** to **20**) and further increase in solubilizing groups (proceeding from **23** to **22**) results in no change in oxidation potential; these results, which suggest electron density at the metal is particularly sensitive to adjacent ring modification, are consistent with those seen upon nitro group incorporation into such complexes (across the series **19**−**30**, oxidation potential is significantly higher for complexes in which the nitro group is attached to the ring adjacent to the metal, namely, **25** and **28**). These results suggest that the effect of π-bridge lengthening on ease of oxidation should only be assessed with complexes incorporating the same number of solubilizing groups. With this in mind, the present data suggest π-bridge lengthening (proceeding from **28** to **29** and then **30**, from **20** to **23**, and from **22** to **24**) progressively increases the ease of oxidation until the tri(phenyleneethynylene) is reached, after which the oxidation potential is invariant.

Absorption maxima and intensities from electronic spectra are collected in Table 2, and the evolution in optical spectra on systematic structural modification is illustrated in Figures 2−5. Incorporating solubilizing groups on the ring adjacent to the metal (proceeding from **29** to **19**) results in a red-shift and decrease in intensity of the absorption bands (Figure 2), while introducing the solubilizing groups at a more remote ring (proceeding from **30** to **20**) results in a decrease in intensity of the higher energy bands (Figure 3); a further increase in number of solubilizing groups remote from the metal (proceeding from **23** to **22**) results in a slight increase in intensity of bands, but again little shift in the location of the absorption maxima (Figure 4). Minimizing solubilizing substituents while π-bridge lengthening, in proceeding from **28**, through **29**, **30**, and **23**, to **24** (Figure 5), results in a distinct blue-shift from the mono(phenyleneethynylene) **28** to the tri(phenyleneethynylene) **30**, with little further change in ν_{max}, but an increase in absorptivity, in proceeding to the penta(phenyleneethynylene) **24**. Closer inspection of the spectra reveals that the next-higher-energy bands red-shift and gain in intensity on chain-lengthening, to eventually coalesce with the lowest energy band for **23** and **24**.

Table 3. Computed Significantly Allowed Single-Photon Transitions (those with oscillator strengths exceeding $f = 0.3$ au) for $[Ru](C_2C_6H_4)_iC_2C_6H_4NO_2$ ($i = 1-4$), Obtained through PBE/TZP and LB94/TZP//PBE/TZP Calculations

		PBE/TZP						LB94/TZP					
model complex[a]	symm[b]	n[c]	E/eV[d]	f/au[e]	occ.[f]	virt.[f]	wt %[g]	n[c]	E/eV[d]	f/au[e]	occ.[f]	virt.[f]	wt %[g]
19M	A_1	1	1.533	0.43	$^{14}B_2$	$^{15}B_2$	94	1	1.167	0.35	$^{14}B_2$	$^{15}B_2$	92
	A_1	3	2.810	0.81	$^{14}B_2$	$^{16}B_2$	74	3	2.441	0.67	$^{14}B_2$	$^{16}B_2$	44
20M	A_1	1	1.112	0.33	$^{17}B_2$	$^{18}B_2$	97	1	0.749	0.30	$^{17}B_2$	$^{18}B_2$	96
	A_1	3	2.162	0.83	$^{17}B_2$	$^{19}B_2$	88	3	1.870	0.78	$^{17}B_2$	$^{19}B_2$	65
	A_1	5	2.975	1.01	$^{14}B_2$	$^{18}B_2$	42	5	2.527	0.34	$^{14}B_2$	$^{18}B_2$	65
	A_1							7	2.801	0.70	$^{17}B_2$	$^{20}B_2$	70
	A_1							10	3.206	0.36	$^{15}B_2$	$^{19}B_2$	49
23M	A_1	3	1.755	0.69	$^{20}B_2$	$^{22}B_2$	93	3	1.507	0.62	$^{20}B_2$	$^{22}B_2$	84
	A_1	6	2.568	0.46	$^{17}B_2$	$^{21}B_2$	47	5	2.086	0.34	$^{17}B_2$	$^{21}B_2$	75
	A_1	5	2.495	0.84	$^{20}B_2$	$^{23}B_2$	75	6	2.244	0.20	$^{20}B_2$	$^{23}B_2$	79
	A_1	7	2.657	0.48	$^{19}B_2$	$^{22}B_2$	56	7	2.326	0.84	$^{19}B_2$	$^{22}B_2$	73
	A_1	8	2.947	0.52	$^{18}B_2$	$^{22}B_2$	57	9	2.695	0.76	$^{18}B_2$	$^{22}B_2$	53
24M	A_1	3	1.514	0.32	$^{22}B_2$	$^{24}B_2$	95	2	1.034	0.13	$^{22}B_2$	$^{24}B_2$	96
	A_1	2	1.490	0.49	$^{23}B_2$	$^{25}B_2$	95	3	1.264	0.41	$^{23}B_2$	$^{25}B_2$	94
	A_1	4	1.942	0.38	$^{21}B_2$	$^{24}B_2$	82	4	1.393	0.10	$^{21}B_2$	$^{24}B_2$	85
	A_1	6	2.282	0.74	$^{20}B_2$	$^{24}B_2$	64	5	1.764	0.28	$^{20}B_2$	$^{24}B_2$	79
	A_1	5	2.112	0.48	$^{23}B_2$	$^{26}B_2$	84	6	1.876	0.38	$^{23}B_2$	$^{26}B_2$	89
	A_1	7	2.346	0.76	$^{22}B_2$	$^{25}B_2$	66	7	2.064	0.88	$^{22}B_2$	$^{25}B_2$	80
	A_1	8	2.620	0.98	$^{21}B_2$	$^{25}B_2$	44	9	2.374	0.90	$^{21}B_2$	$^{25}B_2$	42
	A_1	10	2.797	0.15	$^{22}B_2$	$^{26}B_2$	19	12	2.620	1.01	$^{22}B_2$	$^{26}B_2$	56

[a] Notation used for calculation on model compounds is consistent with that indicated in the main text. [b] Symmetry classification of the identified transition. [c] Energy ranking of the identified transition within the indicated symmetry classification. [d] Calculated transition energy in electronvolts, at the indicated level of theory. [e] Calculated transition oscillator strength, in atomic units, at the indicated level of theory. [f] Principal pair of occupied and virtual orbitals involved in the identified transition. [g] Percentage contribution of principal-orbital character to the calculated transition, at the indicated level of theory.

Theoretical Studies. Our TD-DFT calculations on the four model compounds $[Ru](C_2C_6H_4)_iC_2C_6H_4NO_2$ ($i = 1-4$) delivered, for each model, the 50 lowest energy symmetry-allowed single-photon transitions. Of this number, only a handful of calculated transitions for each model (all such transitions being of A_1 symmetry for the C_{2v}-constrained models) have expectation values f greater than about 0.3 atomic unit (see Table 3).

Orbital characteristics for models **19M**, **20M**, **23M**, and **24M** show considerable common features, as is to be expected from their structural similarity. The HOMO in each case ($^{11+3i}B_2$) is dominated by acetylenic character concentrated on the C_2 unit immediately adjacent to Ru, while the LUMO ($^{12+3i}B_2$) is characterized by C═N bonding of the terminal phenylene to the nitro group. The next few lower lying B_2-symmetry occupied orbitals show acetylenic character at progressively greater separation from Ru at increasing distance from the "frontier", while the next few higher lying B_2-symmetry virtual orbitals are cumulenic in character, associated with C_2 units that are closer to the Ru as the orbital energy increases above the LUMO.

Perhaps because the spatial separation of domains for the HOMO and LUMO becomes more exaggerated as chain length i is increased, the LUMO←HOMO excitation $^1A_1$ becomes progressively less important with increasing i, with the calculated f value for this transition decreasing monotonically at both the PBE/TZP and LB94/TZP levels of theory. Instead, there is a marked tendency toward the strongest transitions being those where there is a close spatial correspondence between the occupied and virtual domains.

Analysis of the TD-DFT results is hampered by inconsistencies between the intensities calculated at the PBE/TZP level of theory and those obtained at the LB94/TZP level.[133] For example, for **24M** (see Figure 6) the most intense transitions at the PBE/TZP level of theory are $^6A_1$ ($^{24}B_2 \leftarrow\!\!- {}^{20}B_2$), $f = 0.74$ au; $^7A_1$ ($^{22}B_2 \leftarrow\!\!- {}^{25}B_2$), $f = 0.76$ au; and $^8A_1$ ($^{21}B_2 \leftarrow\!\!- {}^{25}B_2$), $f = 0.98$ au. For the same compound according to LB94/TZP, the latter two transitions (here $^7A_1$ and $^9A_1$) are again calculated to be intense, with f values of 0.88 and 0.90, very close to the PBE/TZP results. However, the transition involving $^{24}B_2 \leftarrow\!\!- {}^{20}B_2$ character, here $^5A_1$, has a much lower intensity ($f = 0.28$), while the most intense transition according to LB94/TZP, A_1 ($^{22}B_2 \leftarrow\!\!- {}^{26}B_2$), $f = 1.01$ au, has only a weak counterpart ($f = 0.15$) in the PBE/TZP calculations. While the two TD-DFT methods employed yield somewhat inconsistent results for the identities of the most intense single-photon transitions, it remains notable that the most intense transitions consistently display

(121) Touchard, D.; Haquette, P.; Pirio, N.; Toupet, L.; Dixneuf, P. H. *Organometallics* **1993**, *12*, 3132.
(122) Hodge, A. J.; Ingham, S. L.; Kakkar, A. K.; Khan, M. S.; Lewis, J.; Long, N. J.; Parker, D. G.; Raithby, P. R. *J. Organomet. Chem.* **1995**, *488*, 205.
(123) Ge, Q.; Hor, T. *Dalton Trans.* **2008**, 2929.
(124) Fondum, T. N.; Green, K. A.; Randles, M. D.; Cifuentes, M. P.; Willis, A. C.; Teshome, A.; Asselberghs, I.; Clays, K.; Humphrey, M. G. *J. Organomet. Chem.* **2008**, *693*, 1605.
(125) Gauthier, N.; Olivier, C.; Rigaut, S.; Touchard, D.; Roisnel, T.; Humphrey, M. G.; Paul, F. *Organometallics* **2008**, *27*, 1063.
(126) Fillaut, J.-L.; Andries, J.; Marwaha, R. D.; Lanoe, P.-H.; Lohio, O.; Toupet, L.; Williams, J. A. G. *J. Organomet. Chem.* **2008**, *693*, 228.
(127) Onitsuka, K.; Ohara, N.; Takei, F.; Takahashi, S. *Dalton Trans.* **2006**, 3693.
(128) Lavastre, O.; Fiedler, J. *Organometallics* **2006**, *25*, 635.
(129) Wong, W.-Y.; Wong, C.-K.; Lu, G.-L. *J. Organomet. Chem.* **2003**, *671*, 27.
(130) Rigaut, S.; Perruchon, J.; Le Pichon, L.; Touchard, D.; Dixneuf, P. H. *J. Organomet. Chem.* **2003**, *670*, 37.
(131) Fillaut, J.-L.; Perruchon, J. *Inorg. Chem. Commun.* **2002**, *5*, 1048.
(132) Wong, C.-Y.; Che, C.-M.; Chan, M. C. W.; Han, J.; Leung, K.-H.; Phillips, D. L.; Wong, K.-Y.; Zhu, N. *J. Am. Chem. Soc.* **2005**, *127*, 13997.
(133) The problems of selecting the most appropriate functional for predicting absorption spectra using TD-DFT have been discussed recently. See, for example: (a) Jacquemin, D.; Perpète, E. A.; Scuseria, G. E.; Ciofini, I.; Adamo, C. *J. Chem. Theory Comput.* **2008**, *4*, 123. (b) Peach, M. J. G.; Benfield, P.; Helgaker, T.; Tozer, D. J. *J. Chem. Phys.* **2008**, *128*, 044118. (c) Peach, M. J. G.; Le Sueur, C. R.; Ruud, K.; Guillaume, M.; Tozer, D. J. *Phys. Chem. Chem. Phys.* **2009**, *11*, 4465.

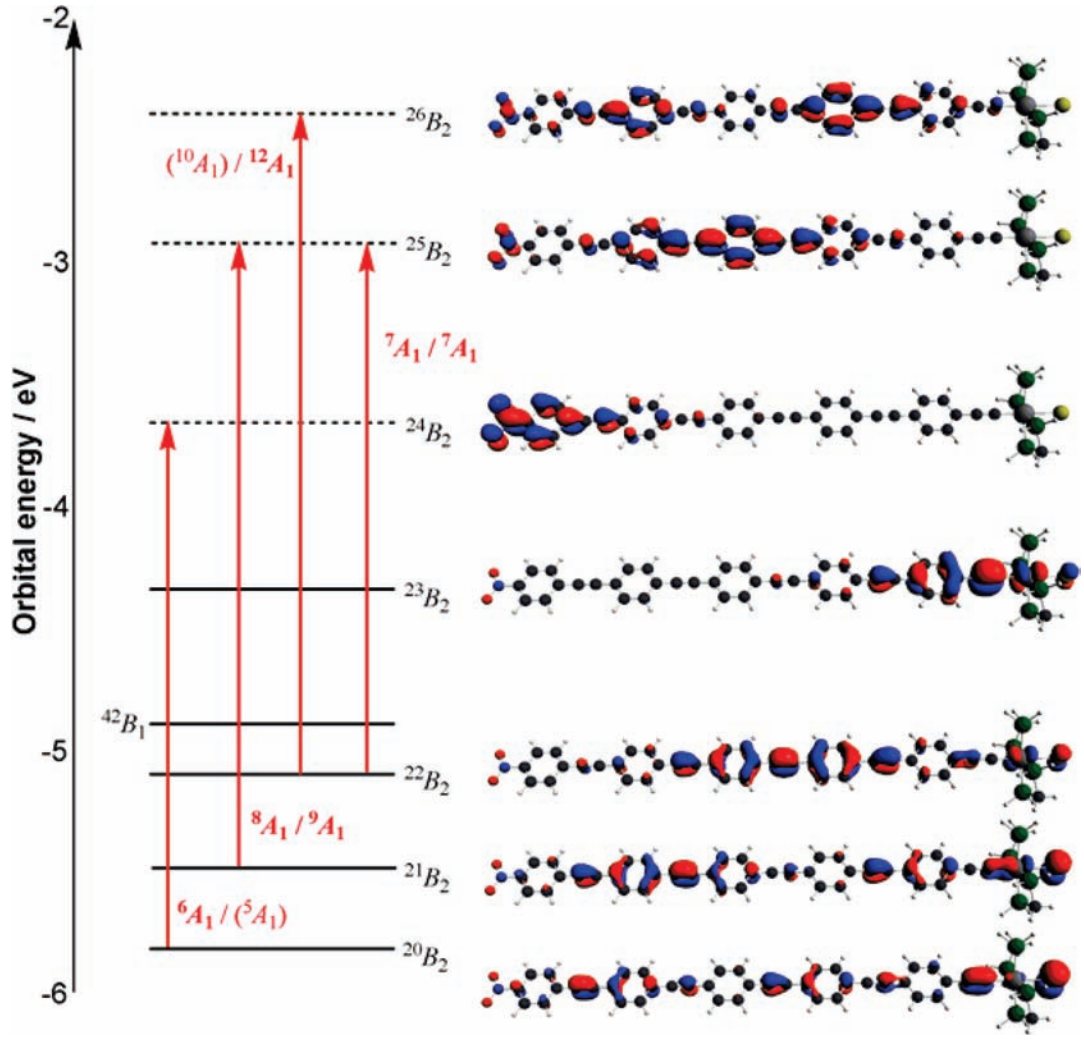

Figure 6. Energy-level diagram (obtained at the PBE/TZP level of theory) and orbital diagram for calculated intense single-photon transitions of the model compound **24M**. Transition term values are shown for the PBE/TZP and LB94/TZP levels of theory, respectively; a term value in parentheses indicates that the transition in question is not notably intense ($f < 0.3$ au) at the indicated level of theory. A common feature of these intense transitions is the generally close spatial correspondence between the electronic domains of the relevant occupied (solid line) and virtual (dotted line) orbitals. All of the transitions identified as intense have excitation energies, at the PBE/TZP level of theory, of 2.0 eV ($\sim$16 000 cm^{-1}) or higher. In contrast, the HOMO−LUMO gap is much less, only 0.73 eV ($\sim$6000 cm^{-1}), but does not feature significant overlap between occupied and virtual domains and is calculated to contribute only weakly ($f \sim 0.1$ au) to the single-photon excitation spectrum of **24M**.

strong domain-region overlap between the identified occupied and virtual orbitals. An apparent consequence of the increasing importance of this effect with increasing chain length is that the frequencies of the most intense transitions do not decrease as rapidly as does the HOMO/LUMO energy separation. Indeed, as the crucial orbitals are displaced progressively more from the frontier, it may well appear that the important transitions become blue-shifted on chain lengthening.

A second mechanism also exists whereby the most prominent transitions detected can appear to blue-shift on chain lengthening. While the lowest energy conformer for **24M**, as for all of its smaller congeners, features coplanarity of all of the coaxial aryl rings, the barriers to intramolecular rotation along any of the ethynyl spindles are not large, with the calculated rotational transition states lying typically 10 kJ mol^{-1}, or less, above the all-coplanar conformer.[134] Further, while the primary effect of moderate on-axis aryl rotation (i.e., for dihedral angle values of up to 30°) is generally to reduce the energy of each allowed transition by a modest quantity (i.e., by 300 cm^{-1} or less), there is a more prominent effect on the calculated oscillator strength for each transition, with internal rotation dampening some transitions and strengthening others. This phenomenon can lead to apparent blue-shifting on chain lengthening (since increasing chain length corresponds to an increase in the number of opportunities for on-axis aryl rotation) when rotation enhances the relative strength of a higher energy transition relative to its lower energy neighbor. Since the spectral features observed in the laboratory are typically broad ($\sim$5000 cm^{-1} fwhm or similar), a rotationally mediated change in the relative intensity of two or more close-lying transitions may well manifest as the blue-shifting of a single broad peak effectively enveloping several transitions.

It is important to note that, while both of these phenomena can result in blue-shifting on chain lengthening, neither effect is exactly systematic: they therefore appear to be of little predictive value. However, they provide a rationalization for the somewhat counterintuitive observation that elongation of the phenyleneethynylene "axis" can result in an increase in the frequency of the observed spectral peak.

Quadratic Nonlinear Optical Studies. The quadratic nonlinearities of **19**−**24** have been determined at 1064 nm; these results, together with previously reported measurements for the

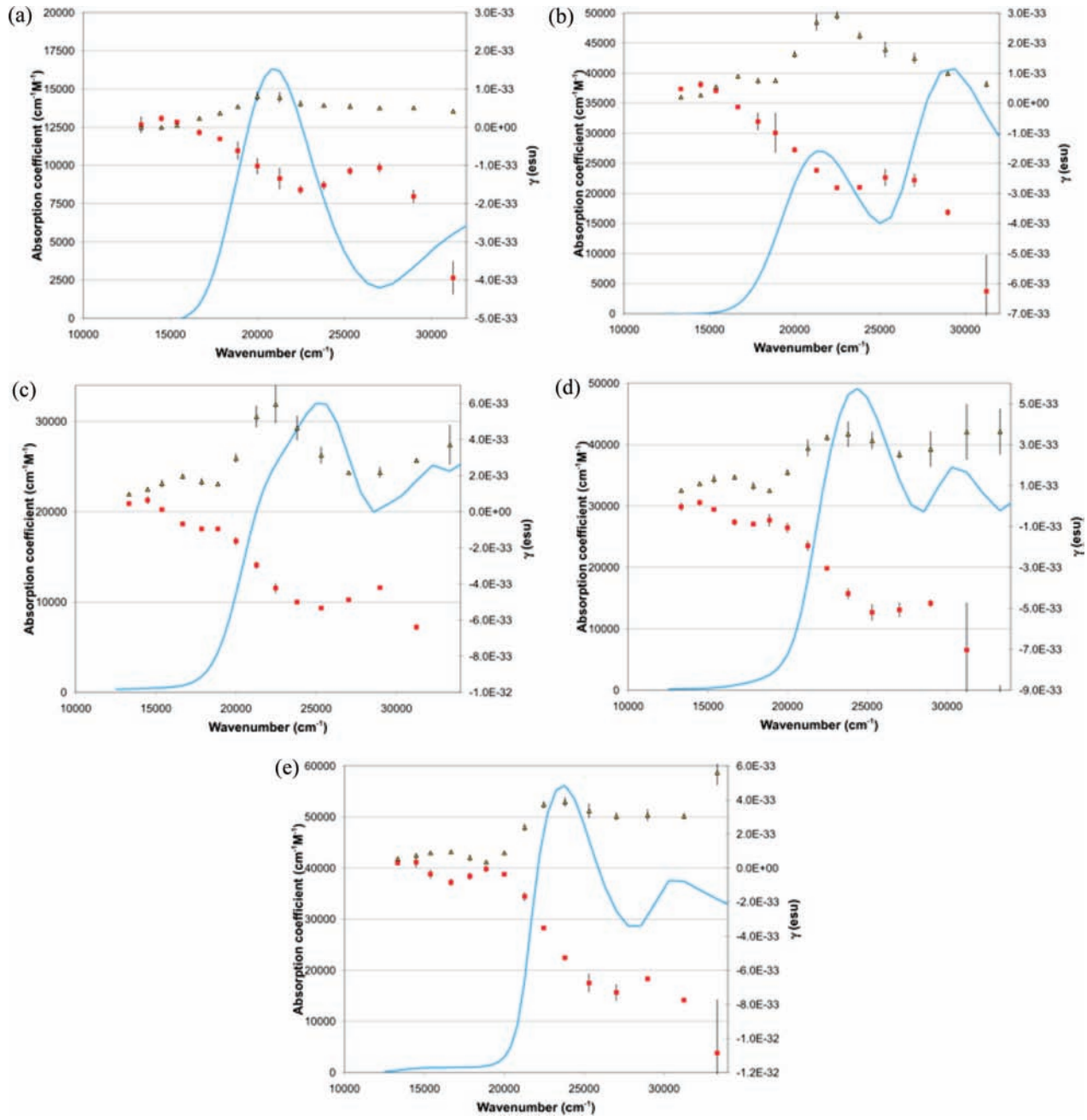

Figure 7. Comparison of the dispersion of the complex hyperpolarizability of (a) *trans*-[Ru(4-C≡$CC_6H_4NO_2$)Cl(dppm)$_2$] (**28**), (b) *trans*-[Ru(4,4′-C≡CC_6H_4C≡$CC_6H_4NO_2$)Cl(dppm)$_2$] (**29**), (c) *trans*-[Ru{4,4′,4″-C≡CC_6H_4C≡CC_6H_2[2,5-(OEt)$_2$]C≡$CC_6H_4NO_2$}Cl(dppm)$_2$] (**20**), (d) *trans*-[Ru{4,4′,4″,4‴-C≡CC_6H_4C≡CC_6H_4C≡CC_6H_2[2,5-(OEt)$_2$]C≡$CC_6H_4NO_2$}Cl(dppm)$_2$] (**23**), and (e) *trans*-[Ru{4,4′,4″,4‴,4⁗-C≡CC_6H_4C≡CC_6H_4C≡CC_6H_2[2,5-(OEt)$_2$]C≡CC_6H_2[2,5-(OEt)$_2$]C≡$CC_6H_4NO_2$}Cl(dppm)$_2$] (**24**), with the one-photon absorption spectra of the compounds (real component: solid squares; imaginary component: open triangles). Note that the hyperpolarizability values were plotted against twice the measurement wavenumber. This permits comparison of two-photon absorption (represented here as the imaginary part of the hyperpolarizability) with one-photon absorption to the same final state.

related complexes **25**−**30**, are presented in Table 2. The major focus of the present study is to assess the impact of π-bridge lengthening upon optical properties. For the dppe-containing complexes, π-bridge lengthening, in proceeding from **25** to **26**, **27**, and finally **21**, results in nonlinearity peaking at the tri(phenyleneethynylene)-containing complex **27**, but there are insufficient data to deconvolute the influence of the ethoxy substituents introduced into **21** to ensure sufficient solubility. We have a more extensive set of dppm-containing complexes that permit further comment. Introduction of solubilizing groups (proceeding from **29** to **19**, or **30** to **20**) results in a ca. 30% reduction in β_{1064}, while further increasing the ethoxy content (proceeding from **23** to **22**) results in no further change, within the error margins. There is sufficient data to offer a comment on the effect on β of π-bridge lengthening; proceeding from **28** to **29**, and then **30** (no ethoxy substituents), **20** to **23** (two ethoxy substituents), and **22** to **24** (four ethoxy substituents) suggests that β peaks at the tri(phenyleneethynylene) stage, after which a saturation effect is apparent.

Table 2 also contains a more limited set of data at 1300 nm and two-level-corrected values for the two wavelengths. The results for the former are in contrast to those at 1064 nm. Introducing solubilizing substituents, in proceeding from **29** to **19**, results in an increase in nonlinearity, while a further increase

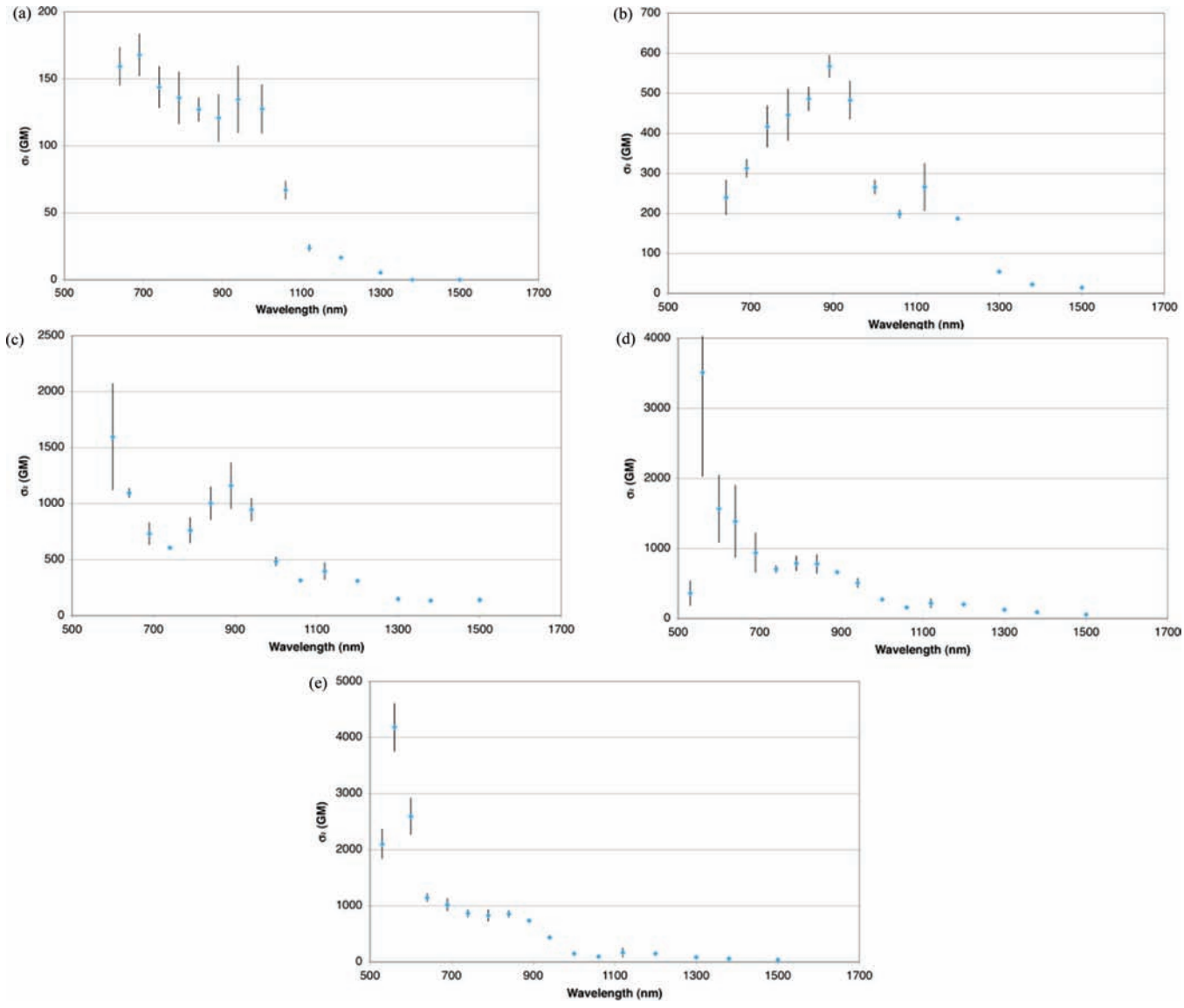

Figure 8. Comparison of the two-photon absorption dispersion of (a) *trans*-[Ru(4-C≡$CC_6H_4NO_2$)Cl(dppm)$_2$] (**28**), (b) *trans*-[Ru(4,4′-C≡CC_6H_4C≡$CC_6H_4NO_2$)Cl(dppm)$_2$] (**29**), (c) *trans*-[Ru{4,4′,4″-C≡CC_6H_4C≡CC_6H_2[2,5-(OEt)$_2$]C≡$CC_6H_4NO_2$}Cl(dppm)$_2$] (**20**), (d) *trans*-[Ru{4,4′,4″,4‴-C≡CC_6H_4C≡CC_6H_4C≡CC_6H_2[2,5-(OEt)$_2$]C≡$CC_6H_4NO_2$}Cl(dppm)$_2$] (**23**), and (e) *trans*-[Ru{4,4′,4″,4‴,4⁗-C≡CC_6H_4C≡CC_6H_4C≡CC_6H_2[2,5-(OEt)$_2$]C≡CC_6H_2[2,5-(OEt)$_2$]C≡$CC_6H_4NO_2$}Cl(dppm)$_2$] (**24**).

in ethoxy content (proceeding from **23** to **22**) results in a decrease in β value. The π-bridge lengthening does not result in a saturation point being reached, β increasing on proceeding from **28** to **29** (no ethoxy substituents) and **20** to **23** (two ethoxy groups). Two-level-corrected data should be viewed with extreme caution; while the trends are broadly similar to those for the corresponding β_λ values, the shortcomings of the model have been discussed extensively elsewhere (ref 100 and refs therein).

Cubic Nonlinear Optical Studies. The cubic NLO properties of selected complexes were assessed over a wide spectral range (Figure 7), the specific complexes (**20**, **23**, **24**, **28**, **29**) being chosen to ensure sufficient solubility for the Z-scan studies. Figure 7 contains the hyperpolarizabiliy values plotted against twice the measurement wavenumber, to facilitate comparison with the linear optical spectrum included in the figure. The studies were undertaken in essentially transparent regions of the UV−vis−NIR spectra (from 6700 cm^{-1} to the onset of one-photon absorption). A few data were collected with moderate linear absorption, and these consequently have large error factors.

With reference to the results depicted in Figure 7, there is generally an approximate correspondence between the one-photon absorption bands and the main two-photon absorption band. The low-energy nonlinear absorption band shown in Figure 7 in the range ca. 12000−18000 cm^{-1}, and appearing for laser wavelengths of ca. 1100−1500 nm, seems to have a multiphoton character with possible strong contributions from three-photon absorption.

Figure 8 shows the absorptive part of the cubic nonlinearity of the five compounds replotted as the (effective) two-photon cross-section versus wavelength of the incident laser beam, with relevant data being collected in Table 2. The rapid increase of the maximal value of the two-photon cross-section in proceeding from **28**, through **29**, to **20** (at ∼900 nm for all the compounds)

is followed by stabilization of the value in proceeding to the longer π-bridge compounds **23** and **24**.

Discussion

The present studies have afforded a series of OPEs end-functionalized by ligated Ru and nitro groups. Increasing OPE length is associated with decreasing solubility, which at the tetra(phenyleneethynylene) length is sufficiently diminished as to cause problems with chemical synthesis. Alkoxy substituents have been employed to ensure adequate solubility both for chemical synthesis and for NLO studies. Solubilizing groups such as these are not necessarily electronically and optically innocent, and so, recognizing that these groups are essential, we have sought to define their influence. Introducing solubilizing groups at the phenylene adjacent to the metal results in a decrease in E^0_{ox} and a red-shift in the low-energy absorption bands. We have not probed this modification theoretically, but introduction of electron-donating substituents at the bridge phenyl ring adjacent to the ruthenium is expected to increase electron richness at the metal center, and thereby increase ease of oxidation. This substitution will also destabilize the HOMO and SHOMO, which are localized at the metal and adjacent ring, resulting in a red-shift in the optical absorption maximum. Introducing solubilizing groups at rings remote from the metal center results in a much smaller red-shift in the optical absorption maximum and does not affect the ease of oxidation, consistent with the aforementioned HOMO/SHOMO localization. Incorporation of these solubilizing groups results in a ca. 30% reduction in β_{1064} and β_0. The calculations are consistent with the dominant charge-transfer transition (which would be expected to contribute significantly to the observed nonlinearity) being metal-to-bridge in character and with a diminished importance of this transition on solubilizing group incorporation and thereby a decreased nonlinearity.

The π-bridge length-dependent evolution of optical properties in organic oligomers has been of considerable interest.[134,135] Poly(phenyleneethynylene)s have potential as photoluminescence or nonlinear optical materials or as fluorescent chemosensors, and monodisperse examples of a wide range of lengths have been prepared.[136−138] Related to the present work, a series of OPEs end-functionalized by di(dodecyl)amino and nitro groups has been examined, with the linear optical absorption maximum blue-shifting on chain-length increase until the trimer is reached, further π-system lengthening leaving λ_{max} invariant.[139] Third-harmonic generation studies of these dialkylamino-nitro-substituted OPEs were hampered by solubility problems.[140] The present studies expand the scope of donor−acceptor-functionalized OPEs to include examples incorporating a ligated metal center. The blue-shift of λ_{max} on chain-lengthening this metal-containing system mirrors that seen in the examples above. Our theoretical studies have identified two possible sources of the observed blue-shift of λ_{max} on chain-lengthening: decreasing importance of the LUMO ← HOMO transition and on-axis aryl rotation-mediated change in the relative intensities of two or more close-lying transitions.

The major outcome of the present work has been to define the effective saturation length of OPE examples end-functionalized by ligated metal and nitro group (donor-bridge-acceptor arylalkynylruthenium complexes), for which metal-centered oxidation potential, linear optical absorption maximum, quadratic optical nonlinearity assessed by HRS at 1064 nm, and two-photon-absorption cross-section assessed by Z-scan all plateau at the tri(phenyleneethynylene) complex. These studies have therefore afforded the specific bridge length for the most efficient optical materials with this metal-containing donor group, as well as providing an interesting comparison of saturation length with related, purely organic, compounds.

Acknowledgment. We thank the Australian Research Council (M.G.H., M.P.C., M.S., R.S.), the Fund for Scientific Research-Flanders (FWO-Vlaanderen; FWO G.0312.08) (K.C.), the Katholieke Universiteit Leuven (GOA/2006/03) (K.C.), and Wroclaw University of Technology (M.S.) for support of this work. M.G.H. is an ARC Australian Professorial Fellow. B.B. thanks King Abdulaziz University for sponsorship.

Supporting Information Available: List of authors of ref 108, the syntheses of compounds **1**−**18** and complexes **20**−**24**, and a cif file giving solution and refinement details and tables of atomic coordinates, bond lengths, and bond angles for the X-ray structural study of **19**. This material is available free of charge via the Internet at http://pubs.acs.org.

JA902793Z

(134) A blue-shift in absorption maximum in related phenyleneethynylene-containing compounds has been noted and discussed. See: (a) Biswas, M.; Nguyen, P.; Marder, T. B.; Khundkar, L. R. *J. Phys. Chem. A* **1997**, *101*, 1689. (b) Beeby, A.; Findlay, K.; Low, P. J.; Marder, T. B. *J. Am. Chem. Soc.* **2002**, *124*, 8280. (c) Siddle, J. S.; Ward, R. M.; Collings, J. C.; Rutter, S. R.; Porrès, L.; Applegarth, L.; Beeby, A.; Batsanov, A. S.; Thompson, A. L.; Howard, J. A. K.; Boucekkine, A.; Costuas, K.; Halet, J.-F.; Marder, T. B. *New J. Chem.* **2007**, *31*, 841. (d) Reference 64.
(135) Martin, R. E.; Diederich, F. *Angew. Chem., Int. Ed.* **1999**, *38*, 1350.
(136) Jones, L.; Schumm, J. S.; Tour, J. M. *J. Org. Chem.* **1997**, *62*, 1388.
(137) Bunz, U. H. *Chem. Rev.* **2000**, *100*, 1605.
(138) Luther-Davies, B.; Samoc, M. *Curr. Opin. Solid State Mater. Sci.* **1997**, *2*, 213.
(139) Meier, H.; Mühling, B.; Kolshorn, H. *Eur. J. Org. Chem.* **2004**, 1033.
(140) Koynov, K.; Bahtiar, A.; Bubeck, C.; Mühling, B.; Meier, H. *J. Phys. Chem. B* **2005**, *109*, 10184.